Published in final edited form as:
Toxicol Pathol. 2009 ; 37(4): 395–414. doi:10.1177/0192623309335060.

Histology Atlas of the Developing Mouse Heart with Emphasis on E11.5 to E18.5

Saija M. Savolainen, **Julie F. Foley**, and **Susan A. Elmore**
NIEHS, Cellular and Molecular Pathology Branch, Research Triangle Park, North Carolina, USA

Abstract

In humans, congenital heart diseases are common. Since the rapid progression of transgenic technologies, the mouse has become the major animal model of defective cardiovascular development. Moreover, genetically modified mice frequently die in utero, commonly due to abnormal cardiovascular development. A variety of publications address specific developmental stages or structures of the mouse heart, but a single reference reviewing and describing the anatomy and histology of cardiac developmental events, stage by stage, has not been available. The aim of this color atlas, which demonstrates embryonic/fetal heart development, is to provide a tool for pathologists and biomedical scientists to use for detailed histological evaluation of hematoxylin and eosin (H&E)-stained sections of the developing mouse heart with emphasis on embryonic days (E) 11.5–18.5. The selected images illustrate the main structures and developmental events at each stage and serve as reference material for the confirmation of the chronological age of the embryo/early fetus and assist in the identification of any abnormalities. An extensive review of the literature covering cardiac development pre-E11.5 is summarized in the introduction. Although the focus of this atlas is on the descriptive anatomic and histological development of the normal mouse heart from E11.5 to E18.5, potential embryonic cardiac lesions are discussed with a list of the most common transgenic pre- and perinatal heart defects. Representative images of hearts at E11.5-15.5 and E18.5 are provided in Figures 2-4, 6, 8, and 9. A complete set of labeled images (Figures E11.5-18.5) is available on the CD enclosed in this issue of Toxicologic Pathology. All digital images can be viewed online at https://niehsimages.epl-inc.com with the username “ToxPath” and the password “embryohearts.”

Keywords

heart; embryo; mouse; in utero lethality

Introduction

In humans, congenital heart diseases occur in approximately twelve out of 1000 live births (Hoffman et al. 2004). Although heart development in all vertebrates, from fishes to humans, follows the same general pattern, much of the pioneering research on the developing heart has been conducted in zebra fish and chicks. Since the rapid progression of transgenic technologies, the mouse has become the major animal model in which to study normal and abnormal cardiovascular development. Because cardiogenesis is a very complicated process and vital to the survival of the embryo, one of the main and relatively common causes of in utero lethality of any post-implantational mutant mouse embryo/early fetus is defective cardiovascular development (Conway et al. 2003; Copp 1995; Papaionnou and Behringer 2005). Currently,

Address correspondence to: Susan Elmore, NIEHS, P.O. Box 12233, Research Triangle Park, NC 27709, USA; elmore@niehs.nih.gov.
Address additional CD requests to: Beth Mahler: mahler1@niehs.nih.gov.

phenotyping the embryonal mouse heart is an arduous task due to limited resources. Current resources include a detailed, descriptive anatomical histology atlas of mouse development (Kaufman 1992; Theiler 1972), an online tutorial of normal mammalian development using scanning electron micrographs (Sulik and Bream 1999), a high-resolution magnetic resonance histology atlas of the embryonic and neonatal mouse (Petiet et al. 2008) and the Edinburgh 3D mouse embryo anatomy atlas (http://genex.hgu.mrc.ac.uk/). However, there is a need for a more detailed, stage-by-stage, descriptive anatomic and histological reference on the developing mouse heart. Because of the potential for strain differences when evaluating normal development or developmental defects, it is crucial to always compare to concurrent controls, with littermates considered the ideal source of comparison.

Early Mouse Heart Development

The heart is the first organ to develop and function in the embryo. Cardiomyocytes differentiate from precursor cells in the primitive streak and move anterior-laterally to form bilateral paired cardiogenic plates (myocardial primordial) in the mouse embryo at E7.5. Subjacent to these plates, endothelial cells differentiate and form right and left endocardial heart tubes (Kaufman and Bard 1999). These endothelial-lined vessels align in a parallel fashion with each other and then fuse across the ventral midline to form a single beating heart tube by E8.0 with rostral arterial (aortic sac) and caudal venous poles (right and left sinus horns). At first, the contractions are irregular, but by E9.0 a regular heartbeat is established. The venous pole acts as the initial pacemaker, and the wave of muscle contraction is then propagated along the tubular heart (Kaufman and Navaratnam 1981).

The heart tube consists of the outer myocardial and the inner endothelial cell layers. Between these two layers is a space filled with an extracellular matrix, the cardiac jelly (DeHaan 1965; Kaufman and Navaratnam 1981; Wessels and Markwald 2000). The heart tube subsequently loops to the right during E8.5–10.5, with the venous pole moving cranially and dorsally (Figure 1). At E8.5, three regions can be distinguished by the bulging morphology: bulbus cordis (future right ventricle), primitive left ventricle, and common atrial chamber behind the primitive left ventricle (Figure 1A) (Kaufman and Bard 1999). Concomitantly with the rightward looping, lengthening of the tube and further ballooning of the future chambers takes place. Myocardium from the pharyngeal arch region (second or anterior heart field) adds to the lengthening outflow tract after the formation of the initial heart tube (first heart field) (Kirby 2002; Kirby 2007; Yelbuz et al. 2002). From E9.5, several segments can be distinguished (Figure 1B). The right and left sinus horns empty all of the systemic blood into the common atrial chamber. The common atrial chamber is connected to the primitive left ventricle by an atrioventricular canal. The primitive left ventricle communicates with the future right ventricle via the bulboventricular canal. The outflow tract, conus and truncus (arteriosus), connects the future right ventricle to the aortic sac. Further development of the atrial and ventricular parts is dependent on the expansion or ballooning of the chambers. The atrial chambers expand on both sides of the developing arterial pole, whereas ventricular chambers form in the ventricular loop along the outer curvature (Figure 1C), with the ballooning producing the interventricular septum between the pouches (Anderson et al. 2006).

In the atrioventricular canal and in the common outflow tract, localized swellings of the inner heart wall arise at E9.5 (Kisanuki et al. 2001; Mjaatvedt and Markwald 1989). These swellings are termed atrioventricular and outflow tract cushions or ridges, and they will contribute to all septal and valvular structures that are needed to produce the four chambers of the heart as well as the two separate outflow channels, the aorta and the pulmonary trunk, respectively (Fananapazir and Kaufman 1988).

Three populations of extracardiac cells are incorporated into the heart through waves of cell migration: pro-epicardium from the mesenchyme of the septum transversum; dorsal

mesocardium, which is incorporated into the prospective atria from the body wall; and cardiac neural crest cells, which migrate through pharyngeal arches to the outflow tract. The pro-epicardium invests the external surface of the entire heart, including the outflow tract during and right after the looping E9.0-11.0 (Komiyama et al. 1987). In addition, endothelial and smooth muscle cells of the coronary vasculature, as well as connective tissue, are formed by the epithelial-mesenchymal transformation of the epicardium (Perez-Pomares et al. 1997). In addition to forming a primary atrial septum (septum primum), dorsal mesocardium is important in connecting the primitive atrial chamber to the midline of the body of the embryo and to the pulmonary pit, the entrance point of the pulmonary vein (Webb et al. 1999). The cardiac neural crest cells contribute fundamentally to the developing aortic arch arteries and to the septation of the outflow tract and the formation of outflow tract valves (Gitler et al. 2003; Kirby 2007).

Principal Features of Embryonal/Fetal Circulation

By E8.5, the primitive circulation has been established. The inflow of blood to the venous pole of the primitive heart comes from three sources: oxygenated blood from the placenta via the umbilical veins, and deoxygenated blood from the body (via the right and left anterior and posterior cardinal veins, common cardinal veins and horns of sinus venosus) and from the yolk sac (via the vitelline veins) (Kaufman and Bard 1999). The collection point of blood from the two sinus horns is called the sinus venosus, and the junction of the sinus venosus with the primitive atrium is called the sinoatrial junction. As this junction gradually shifts to the right, two craniocaudally oriented valvelike structures, the right and left venous valves, are produced. These valve leaflets will meet cranially and form a septum called the septum spurium, which does not contribute to atrial partitioning (Anderson et al. 2006; Kirby 2007).

At E11, concomitantly with the development of the lungs in the body wall behind the heart, a primary pulmonary vein starts to canalize within the dorsal wall of the common atrial chamber, at the site of the mesocardial pulmonary pit and between the left and right pulmonary ridges (Anderson et al. 2006; Kirby 2007). These ridges demarcate the site of the persisting dorsal mesocardium within the atrial wall. The right pulmonary ridge becomes especially prominent and is the structure that has long been known as the vestibular spine (His 1880).

From the heart, the largely oxygenated blood goes through the outflow tract to the branchial (pharyngeal) arches and then around the primitive pharynx to the dorsal aortae, most of it supplying the rostral regions of the embryo. In the mid-abdominal region, the paired dorsal aortae fuse to form a single midline vessel, which gives off the vitelline artery supplying the primitive yolk sac. More caudally, the single dorsal aorta bifurcates again and gives rise to the common iliac arteries and then the paired umbilical arteries, which carry the deoxygenated blood to the placenta and the various arterial branches to the pelvic viscera.

By the time looping has finished, the aortic sac at the arterial end has given rise to six bilaterally symmetric vessels known as pharyngeal or aortic arch arteries. The pharyngeal arch arteries arise sequentially along the anterior-posterior axis, each traversing a pharyngeal arch before joining to the paired dorsal aortae (Hiruma et al. 2002; Kaufman 1992). The first and second pharyngeal arch arteries develop around E8.5–9.5 but are disrupted by E10.5. However, their distal parts persist in mice and are transformed into the mandibular and stapedial and hyoid arteries, respectively (Hiruma et al. 2002). The third pharyngeal arch arteries are evident at E9.5, and fourth and sixth pharyngeal arch arteries at E10.0 and E10.5, respectively. The fifth pharyngeal arch arteries never fully form in mammals. The arch arteries undergo extensive remodeling to ultimately form a mature aortic arch and proximal pulmonary arteries.

Apoptosis during Heart Development

Programmed cell death, or apoptosis, occurs in the normally developing heart at specific times and regions, and it is involved in the developmental remodeling of tissues by targeting transient cells and allowing for further tissue differentiation (Jacobson et al. 1997). The primary sites of apoptosis in the normal developing heart are the outflow tract and atrioventricular cushions, the walls and developing valves of the aorta and pulmonary trunk, and the upper part of the interventricular septum (Icardo 1996; Pexieder 1975; Poelmann et al. 2000). Apoptosis also plays an essential role in the ventricular morphogenesis (E11.0–16.0) (Abdelwahid et al. 1999). Outside the heart, remodeling of the originally symmetric pharyngeal arch arteries toward the unilateral left-sided aortic arch coincides with a highly spatiotemporal apoptosis pattern (Molin et al. 2002). Though apoptosis is a normal phenomenon in embryonic heart development, aberrant patterns of apoptosis may cause cardiac malformation, including septation and coronary anomalies and interrupted aortic arch segments (Poelmann and Gittenberger-de Groot 2005).

Defective Mouse Heart Development

To date, over a thousand mutant mice with abnormal heart morphology have been reported in the literature (Table 1). A majority of these defects cause lethality during embryonic/early fetal development. Early lethality (E8.5–11.0) may be due to the inadequate establishment of embryonic-maternal circulation, linear heart tube formation defects, and/or poor cardiac function (Conway et al. 2003). The classic sign of poor cardiac function is edema. The progressive fluid build-up within the pericardial cavity may by itself result in further functional defects, and finally lethality. Failure to undergo correct looping and chamber formation of the primitive heart tube is rarely fatal per se, but it may lead to subsequent lethal misalignment defects.

At later stages (E11.0 onward), improper septation of the primitive ventricles and atria, failure to establish the divided outflow tract, or inadequate establishment of the cardiac conduction system may result in embryonic lethality. At birth, failure of the in utero cardiac system to adapt to adult life and close the inter-atrial and aorta-pulmonary trunk shunts may lead to death (Conway et al. 2003). Defects in embryonal/fetal heart development may cause lethality even later in postnatal life. It is also worth noting that a single developmental defect typically results in subsequent additional defects. However, especially in transgenic mice, several unrelated primary defects may arise.

Herein, the further development of the murine heart from E11.5 to E18.5 is described and demonstrated in detail with labeled representative histological images of different stages and orientations.

Materials and Methods

Animals

In this study, CD-1 IGS mice/Crl:CD1(ICR) timed pregnant dams (Charles River Laboratories, Raleigh, NC) were used. All animal procedures used in this study were approved by the National Institute of Environmental Health Sciences Animal Care and Use Committee.

Staging

The morning on which the vaginal plug was found was referred to as E0.5 (also described in the literature as 0.5 days post-conception, or DPC). Since considerable variation occurs in the timing of ovulation and conception and in the developmental status of individual embryos, even in 1 litter, special care was taken to match both the external and internal features of each embryo to the known developmental landmarks (Kaufman 1992). Corresponding Theiler

stages (TS), another staging system widely used for mouse embryos (Theiler 1972; Theiler 1989), are also presented.

Collection of the Embryos

Embryo collection was carried out on the mornings of the designated days (E11.5 to E18.5). Pregnant mice were euthanized by CO_2. Individual embryos were isolated under the dissection microscope from the uterus and extra-embryonic membranes while in cold 0.1 M phosphate buffered saline (PBS), and transferred to Bouin's fixative. The embryos were checked for any signs of external or gross cardiac abnormalities or insufficiency, such as defective placenta, growth retardation, tissue edema, and blood-engorged liver, which were not present in any of these embryos.

Fixation

Embryos were fixed in Bouin's fixative (Poly Scientific, Bay Shore, NY). Fixation time was dependent on the embryonic age: E11.5, two hours; E12.5 to 16.5, four hours; and E17.5 to 18.5, seventy-two hours. In the E18.5 fetuses, a midline incision was made through the thoracic and abdominal cavity to improve penetration of the fixative. Following fixation, embryos were rinsed in 70% ethanol saturated with lithium carbonate (Sigma-Aldrich, St. Louis, MO) for three 30-minute washes and processed for paraffin embedding. Embryos younger than E13.5 were embedded in 1% agar before submission to minimize handling during paraffin embedding. For each time point, embryos were embedded on their backs, sides, or heads for sectioning in the respective coronal (frontal), sagittal, or transverse (horizontal) plane. Serial 6-μm sections through the entire embryo were placed on charged slides (A. Daigger & Co., Vernon Hills, IL) and routinely stained with hematoxylin and eosin (H&E) for histopathologic review.

Scanning

Digital images were captured from H&E-stained slides scanned on the Aperio ScanScope T2 instrument (Vista, CA) using Image Scope software, version 8.2 (Aperio). White balance correction and image resizing were completed using Adobe Photoshop CS3 (Adobe Systems Inc., San Jose, CA).

Heart Development E11.5–18.5

E11.5 (TS19)

Main developmental events:

Progressive septation of the outflow tract

Progressive septation of the atria and ventricles

Outflow Tract Septation—Various terminologies of the different parts of the common outflow tract have been used and were reviewed in Pexieder 1995 and Webb et al. 2003. The undivided outflow tract has three parts: aortic sac, truncus (arteriosus), and conus. During the septation of the common outflow tract, these different parts contribute to the outlets, valves, and bases of the aortic and pulmonary trunks, which are formed by E13.5.

The septation of the common outflow tract occurs by three different mechanisms: the initial division of the aortic sac by the neural crest–derived cells, the septation of the distal part of the outflow tract (truncus) by a septation complex, and the zipperlike closure of the proximal part of the outflow tract (conus) through the fusing of the outflow tract cushions (Kirby 2007). The septation complex consists of two prongs of condensed mesenchyme connected by the shelf of tissue in the aortic sac (Waldo et al. 1998; Waldo et al. 1999, reviewed by Creazzo et al.

1998 and Webb et al. 2003). For the purposes of this paper, the OFT at this stage is defined as the region of the heart tube between the trabeculated part of the right ventricle and the aortic sac, which is subdivided into proximal, intermediate, and distal components, according to the nomenclature established by Fananapazir and Kaufman (1998).

By E11.5, the shelf of neural crest–derived cells has protruded into the dorsal wall of the aortic sac, dividing the distal outflow tract into aortic and pulmonary channels (Figures 11.5B and 11.5E). Proximal to the aortic and pulmonary channels, the aorticopulmonary complex septating the truncus can be seen (Figure 3B), and proximal to the septating truncus, the lumen of the common outflow tract is filled with two spiraling cushions (labeled as OCT), also called conotruncal or bulbar spiral ridges (Figure 11.5D). In the cushion tissue, the luminal endocardial cell layer is distinguishable from the cushion mesenchyme. The two condensations of mesenchymal cells (i.e., aorticopulmonary septation complex) in the future site of fusion can also be seen.

The outflow tract cushions will partly transform into two sets of semilunar valve cusps or leaflets in the dividing truncus. The third cusp of each valve will develop from the mesenchymal tissue of the anterior (future pulmonary) and posterior (future aortic) wall of the truncus, respectively. The earliest anlages of the semilunar outflow tract leaflets are observed at this stage. Figure 2B demonstrates solid tubercles of the pulmonary valve leaflets (labeled as PVL), protruding toward the lumen of the developing pulmonary trunk. Development of the aortic valve leaflets has also started; however, they are not present in this plane of section.

Atrioventricular Canal—Two atrioventricular endocardial cushions are apparent in the atrioventricular canal (Figures 2B and 2D). The inferior atrioventricular cushion is associated with the outer curvature, and a superior atrioventricular cushion with the inner curvature (labeled as IAC and SAC). Along the inner curvature of the heart, outflow tract and atrioventricular cushion systems are in close proximity to each other (Figure 2D). At this stage, the outflow tract arises from the bulbus cordis (future right ventricle) (Figures 11.5F, 11.5G, and 11.5H), whereas the atrioventricular canal originates superior to the bulboventricular canal (Figures 2B and 2C). Relatively small lateral atrioventricular cushions (labeled as RLAC and LLAC) start to develop at this stage (Figure 11.5I).

An important developmental event in the maturation of both the outflow tract and atrioventricular cushions is the endocardial epithelial-to-mesenchymal transformation (Markwald et al. 1977). During this transformation, a subset of endocardial cells delaminates from the luminal epithelium, assumes a mesenchymal phenotype, and migrates into the extracellular matrix of the cushions. Some still round, transformed cells can be seen to migrate from the luminal edge deeper into the cushion tissue (Figure 11.5B2, a higher magnification of 11.5B1 demonstrating the atrioventricular cushions with migrating round transforming cells [arrows]).

A perturbed epithelial-to-mesenchymal transformation may lead to hypo- or hypercellularized cushions, and subsequently to a spectrum of cushion abnormalities (see E12.5; defects in atrioventricular canal septation).

Systemic Veins—By E11.5, the venous drainage has undergone significant rearrangements (Anderson et al. 2006; Kaufman and Bard 1999; Kirby 2007). The right vitelline vein has contributed to the inferior vena cava, which from now on carries deoxygenated blood from the lower body to the heart. The vein called the ductus venosus allows placental oxygenated blood from the left umbilical vein to bypass the liver and flow directly into the inferior vena cava. The left sinus horn has been reduced significantly in size, is now called the left coronary sinus, and is the vein connecting the developing left superior vena cava with the post-hepatic part of

the inferior vena cava. Approximately at this stage, the right sinus horn and the common cardinal vein incorporate into the right atrium, leaving the right superior cardinal vein to contribute to the developing superior vena cava. All these systemic venous tributaries terminate in the inferior vena cava, which enters into the presumptive right atrium via a single opening, namely, the sinus venosus (Figure 11.5A -SV). This sinoatrial junction is guarded by the right and left venous valve leaflets, labeled as VV in Figure 11.5A. The pulmonary vein has canalized in the midline of the body but will drain into the left atrium because the septum primum develops to the right of its entrance site (Figures 13.5I, 15.5I, 17.5D, and 18.5F - PVe).

Atrial Myocardial Wall—Although the roof and lateral walls of the definitive atria are composed of rough-walled atrial appendages (Figures 2B and 2C) derived from the myocardium of the embryonic atrium, the atrial body is recruited from heart muscle cells surrounding the venous junctions (Soufan et al. 2004). Concomitantly with the formation of the muscular mantle around the right sinus horn and common cardinal vein, this myocardium is taken up into the right atrium (Kruithof et al. 2003), whereas the myocardium that has been coalesced around the pulmonary vein becomes integrated into the developing left atrium by E11.5 (Franco et al. 2000; Soufan et al. 2004).

Atrial Septation—The first indication of intra-atrial septation is the formation of the septum primum, which starts to grow from the atrial roof toward the atrioventricular endocardial cushion tissue at E10.0 (Kaufman and Bard 1999).The septum primum is inferiorly continuous with the right pulmonary ridge (vestibular spine), and thus the development of the septum primum confines the newly canalized pulmonary venous orifice to the left atrium (Webb et al. 1998). The leading edge of the septum primum is covered with a mesenchymal cap derived from the dorsal mesocardium, and upon caudal expansion of the septum primum this mesenchymal cap, the vestibular spine, and the atrioventricular cushions fuse at approximately E12.0 (Figure 2C - SP). This mesenchymal junction is later replaced with cardiomyocytes except for the central dense connective tissue structure known as Todaro's tendon (Webb et al. 1998), which will form the anterior extension of the valve of the inferior vena cava. This tendon is a vital structure in demarcating the position of the atrioventricular node (Ho and Anderson 2000). Prior to the extension of the septum primum to the atrioventricular cushions, the communication between the atria is called the ostium primum, labeled as OP in Figure 11.5I. Before the closure of the ostium primum, another opening, the ostium secundum, labeled as OS in Figure 2C, breaks down in the upper part of the septum primum, providing continuity between the right and left atrium. The other inter-atrial septum, the septum secundum, starts to develop at E12.5.

Ventricular Myocardial Wall—Myocardial cells with the characteristic sarcomeric proteins and myofibril assembly are present in the heart tube before the first contractions at E8.5 (Lyons et al. 1990). As the distinct chambers start to form, cardiomyocytes with fully differentiated sarcomeres are found in the ventricular and atrial walls. Proliferation of cardiomyocytes within each chamber is necessary to support the increasing hemodynamic load during embryonic development. The myocardium expands from a thin layer of cells beneath the epicardium to form a thicker, compact zone of muscle (Vuillemin and Pexieder 1989). The most active proliferation, and hence the major increase in thickness of the ventricular wall, occurs between E11.5 and E14 (Erokhina 1968; Kirby 2007), and it is the epicardium that maintains this proliferation (Chen et al. 2002). A subdivision of cardiomyocytes forms specialized structures called trabeculae, which project into the chamber cavity. Trabeculation serves primarily as a means to increase myocardial oxygenation in the absence of coronary circulation (Wessels and Sedmera 2003). The ventricular walls are more trabeculated than the atrial walls. Large ventricular trabeculations are present from E11.0 (Figure 2D - asterisk).

Abnormal regulation of myocardial cell proliferation, particularly the lack of epicardium, will result in a hypoplastic myocardial wall (Figure 10A), muscular ventricular septal defects (VSD), and cardiac failure (Table 1).

Ventricular Septation—The interventricular septum is produced between the future ventricles. This muscular component, derived from the region of ventricular wall adjacent to the bulboventricular groove, labeled as BVG in Figure 11.5I, is apparent at this stage, though the connection between the future ventricles is still open through the bulboventricular canal, labeled as BVC in Figure 11.5D.

E12.5 (TS21)

Main developmental events:

Progressive septation of the outflow tract

Initiation of atrioventricular canal septation

Outflow Tract Septation—By E12.5, septation of the distal portion of the outflow tract, including the semilunar outflow tract valves, has been completed, and the proximal part of the outflow tract septum in the conus starts to close in a zipperlike fashion from distal to proximal toward the ventricles. The aorticopulmonary septation complex does not extend into the conus. Instead, neural crest cells that have already migrated into the conal ridges gather beneath the endocardium, causing the ridges to bulge. When the ridges meet in the middle of the lumen, the endocardium covering the ridges breaks down and the septum is formed by the underlining mesenchyme and myocardium (Waldo et al. 1998; Waldo et al. 1999). This conal septum (Figure 12.5F - COS) separates the subpulmonary and subaortic ventricular outlets, also called pulmonary (infundibulum) and aortic roots (vestibule). The pulmonary root and conal ridges (labeled as OCT) lining it are demonstrated in Figures 3D and 12.5E. In the coronal view from an embryo of a slightly less developed stage, division of the truncus is still underway and the aorticopulmonary septum complex within the outflow tract cushions is distinguishable (Figure 3B - asterisk). The conal cushions are still to be fused to form the septum (Figure 12.5D - OCT).

Atrioventricular Canal—The superior and inferior atrioventricular cushions fuse to form an atrioventricular septum or septum intermedium, which divides the atrioventricular canal into separate right and left canals. The atrioventricular septum is shifted over the interventricular septum, which allows the right and left atrioventricular canals to be aligned with the corresponding ventricles. All the other cardiac septa (conal aspect of the outflow tract septum, interventricular septum, and septum primum) ultimately fuse with the atrioventricular cushions, contributing to the atrioventricular septation (Webb et al. 1998).

The undivided atrioventricular canal (AVC) is apparent in Figure 12.5A. More proximally, the bulging superior and inferior atrioventricular cushions are about to fuse (Figure 12.5B -SAC, IAC). All four atrioventricular cushions contribute to the formation of atrioventricular valves (the right tricuspid and left mitral bicuspid valve) and their supporting structures (Lincoln et al. 2004). The inferior and superior atrioventricular cushions will partly transform to the septal leaflet of the tricuspid valve and the aortic leaflet of the mitral valve, whereas the lateral atrioventricular cushions will give rise to the remaining valve leaflets: the anterior-superior leaflet of the tricuspid valve and the mural leaflet of the mitral valve (Lamers et al. 1995). The four different atrioventricular cushions are apparent in Figure 3C, labeled as SAC, IAC, RLAC, and LLAC.

Hypoproliferation of atrioventricular cushion mesenchyme is associated with atrioventricular canal septation defects, such as a common or complete atrioventricular canal (CAVC), and underdeveloped atrioventricular valve leaflets (Figure 10E). Defects in atrioventricular canal septation may also result in deficient ventricular and atrial septation, termed VSD and atrioventricular septal defect (AVSD), and deficient blood flow between all heart chambers. If the atrioventricular septum forms but fails to shift to the right, both the right and left atrioventricular canals communicate with the left ventricle, resulting in a double-inlet left ventricle (DILV). Since the rate and location of all cushion mesenchyme proliferation are important in formation of the valve apparatus, uncontrolled proliferation of cushion mesenchyme and subsequent thickening of the leaflets is associated with valve defects such as abnormal closure (atresia) or narrowing (stenosis) of the valves. Atrioventricular septal defect combined with atresia of the tricuspid (or mitral) valve results in single-inlet left (or right) ventricle (indicated with arrows in Figure 10F).

Ventricular and Atrial Septation—At E12.5, there is still communication between the two ventricles. The most proximal part of the conal ridges together with the atrioventricular cushions will contribute to the membranous component of the interventricular septum (Figure 3C - IVS) and will close the connection between ventricles by E13.5–14.0. The ostium secundum (Figure 3C - OS) provides communication between the atria after the ostium primum has closed completely.

If the ostium primum fails to close by fusion of the cushion-like cap of the septum primum with the atrioventricular cushions, a primary atrial septal defect will develop. As discussed earlier, this defect is usually associated with insufficient fusion of the atrioventricular cushions, and thus is also called atrioventricular septal defect.

Development of the Systemic Veins—After approximately E12.0, the veins draining the rostral regions of the embryo are called right and left superior venae cavae. The right superior vena cava drains the right side of the head and neck and the right forelimb and empties into the inferior vena cava before entering into the right atrium (Figure 3C). At a later stage of development, the right superior vena cava will have an entrance of its own at the posterior wall of the right atrium. The right and left venous valve leaflets have fused cranially and formed a septum spurium, which demarcates the entrance site of the systemic veins from the rest of the right atrium (Figures 14.5I and 17.5E - SSp).

The left superior vena cava drains the left side of the head and neck and the left forelimb and is connected via the coronary sinus with the inferior vena cava, which has an entrance site just caudal to the floor of the right atrium (Figures 13.5A and 14.5A - LSV). Later, by E15.5, the coronary sinus drains directly into the right atrium (Kaufman and Richardson 2005). This site of entry gradually moves toward the rostromedial wall of the right atrium, whereas the inferior vena cava retains its entrance in the most caudal part of the right atrium.

E13.5 (TS22)

Main developmental events:

Bilaterally asymmetrical aortic arch system

Completely septated outflow tract and ventricles

Remodeling of the atrioventricular cushions

Aortic Arch Development—The systemic blood that enters the right atrium is a mixture of oxygenated blood from the placenta and deoxygenated blood from the body. From the right atrium, the largely oxygenated blood passes (through an inter-atrial opening, at this stage the

ostium secundum) first to the left atrium, and then to the left ventricle and into the systemic circuit through the ascending (thoracic) aorta. The ascending aorta (Figure 4D - AAo) and its branches are directed toward the head and neck regions (via the common carotid arteries) and to the upper limbs (via the left and right subclavian arteries). The blood that fails to proceed to the left atrium passes to the right ventricle and into the pulmonary trunk. Minimal blood from the pulmonary trunk is being directed toward the lungs (via the pulmonary arteries), and the majority passes via the ductus arteriosus to the descending (abdominal) aorta, which is derived from the midline dorsal aorta. The abdominal aorta supplies the tissues and organs of the abdomen and lower limbs as the blood becomes increasingly deoxygenated. This blood then passes via the umbilical arteries to the placenta to be reoxygenated.

By E13.5 the majority of the right-sided dorsal aorta and aortic arch arteries have undergone programmed cell death (apoptosis), leading to the aortic arch system that is almost the same as in the adult mouse (Hiruma et al. 2002; Kaufman 1992; Kaufman and Bard 1999). At this stage, the right horn of the T-shaped aortic sac has been transformed into the right brachiocephalic artery, whereas the left horn together with the left fourth pharyngeal arch artery have developed into the definitive aortic arch (Figures 13.5E and 14.5E - AA). The third arch artery has contributed to the proximal part of the carotid arteries, and the sixth arch artery to the pulmonary trunk, from which the pulmonary arteries to the left and right lungs branch off (Figures 13.5G, 17.5B, and 18.5D - PA), and the ductus arteriosus (Figures 12.5F, 13.5F, 14.5F, 15.5F, and 17.5A - DA).

Development of a correctly remodeled vascular arterial system is required for embryonic viability. Abnormal formation, regression, or persistence of the arch or arch arteries may result in defects such as an abnormal restrictive narrowing of the lumen (coarctation) or interruption of the aortic arch, double aortic arch, or right aortic arch. If the ductus arteriosus fails to close perinatally, the condition is termed patent ductus arteriosus and is lethal.

Completion of the Outflow Tract and Interventricular Septation—Septation of the outflow tract has been completed. At the site of fusion of the conal ridges, there is a fibrous raphe in the wall between the pulmonary and aortic roots (Figure 4D - asterisk), which will be transformed into a muscularized, adult-type septum. This is one of the sites of marked apoptosis in the normal developing heart, and a number of septal mesenchymal cells will undergo apoptosis (Figure 5) prior to the onset of muscularization at E14 (van den Hoff et al. 2004). The former conus region, the bases or roots of the arterial trunks that are recognized as the smooth-walled regions of the ventricles just beneath the pulmonary and aortic semilunar valves, are visible (Figures 13.5E, 13.5H, and 13.5J - PR and 14.5D - AR). This event also completes the septation of the ventricles, since the most proximal part of the conal ridges contributes to the membranous part of the interventricular septum (Figures 4C and 4D - IVS).

During septation, the aorta becomes wedged between the pulmonary trunk and the atrioventricular valves (Figures 13.5A–G, 15.5G - Ao). This wedging is dependent on the retraction or shortening and rotation of the truncal myocardium (Thompson et al. 1987; Watanabe et al. 1998). This event results in the normal alignment of the aorta and pulmonary trunks with the left and right ventricles, respectively.

Abnormalities in septation or incomplete spiraling of the outflow tract result in many congenital cardiac defects. Defect(s) in outflow tract septation will result in persistent truncus arteriosus (PTA) (Table 1, Figure 10B). Absence of neural crest cells is directly associated with the absence of the outflow tract septum, as demonstrated in both avian and mouse models (Jiang et al. 2000;Kirby et al. 1983;Phillips et al. 1987). The abnormal size, position, or shape of the conotruncal ridges and/or subsequent decrease or lack of counterclockwise rotation of the outflow tract will also cause outflow tract septation defects and malalignment of the great

arteries. As a result of the failure of the conal septum to connect to the muscular interventricular septum, PTA, and any misalignment of the conotruncus results in an obligatory (membranous) VSD. The classification of a defect is accomplished by relating the location of the VSD to the origin of the great vessels. In a defect termed overriding aorta, the malaligned root of the aorta is positioned over the VSD (Table 1,Figure 10D). The primary cause of overriding aorta is probably the failure of the addition of myocardium to the outflow tract from the secondary heart field (Farrell et al. 1999). When a dextropositioned aorta overriding a VSD is accompanied by pulmonary valve stenosis and hypertrophy of the right ventricle, the condition is termed tetralogy of Fallot. If the aorta obtains 50% or more of its blood from the right ventricle, the defect is classified as a double-outlet right ventricle (DORV) (Table1, Figure 10C). If the aorta and pulmonary trunk are connected to the wrong ventricles, the defect is called transposition of the great arteries (TGA).

The Outflow Tract and Atrioventricular Valves—Maturation of the semilunar valve leaflets is the last major morphogenetic event with regard to the outflow tract. The pulmonary valve is located at the junction of the right ventricle and the proximal part of the pulmonary trunk (Figure 13.5E - PVL, PT), which is directed toward the left side of the thorax. The aortic valve is located at the junction between the outlet of the left ventricle and the proximal part of the ascending aorta (Figures 13.5G - AVL, Ao), which is directed toward the right. At this stage, the valve leaflets are not yet fully developed. Three leaflets (i.e., thin, triangular flaps) can be distinguished in both the pulmonary and aortic valves (Figure 4B - PVL, Ao). An apoptotic process called excavation takes place in the arterial face of the leaflets during E12.5–15.5, resulting in their final shape and composition (i.e., a core of connective tissue surrounded by the endothelium) (Hurle et al. 1980). Immature semilunar valve leaflets are demonstrated in Figures 12.5B1, 12.5B2 (a high-power image of 12.5B1), 13.5J - AVL, and 6B - AoV, and mature pulmonary and aortic valve leaflets in Figures 15.5E, 16.5B, 18.5B - PVL and 8D - AoV, 9D - AVL, 15.5G - AoV, 16.5C, 16.5D, 17.5C, 17.5F - AVL, 18.5C1, 18.5C2-AoV, AVL (a higher magnification of 18.5C1).

Between E11.5–13.5 the atrioventricular valve leaflets grow significantly due to mesenchymal cell proliferation. At this stage, the leaflets of both the tricuspid and mitral valves seem to be elongated and pressed closely against each other (Figure 4C - TVL, MVL). A process of myocardial delamination separates the lower part of the atrioventricular valve leaflets from the myocardial wall and the interventricular septum, resulting in freely moveable, bilayered leaflets (Figures 13.5I1 and 13.5I2 - MVL, a higher magnification of 13.5I demonstrating the delaminated mitral valve leaflets).

Pericardium—(Parietal) pericardium, the outer portion of the sac covering the heart, is mainly composed of connective tissue (Figure 4C - PC). The pericardium is firmly attached posteriorly to the diaphragm, laterally to the mediastinal pleura, and ventrally to the sternum. Epicardium (visceral pericardium) is the outermost cell layer of the heart and invests the heart by E11.0. The space between the pericardium and epicardium is called the pericardial cavity (Figure 4C - PCC).

E14.5 (TS23)

Main developmental event:

Atrial septation complete

Outflow Tract and Interventricular Septation—The fibrous raphe at the site of fusion of the OFT ridges in the wall between the pulmonary and aortic roots is still present (Figures 14.5C, 14.5F, and 6D - asterisk). The line of closure of the interventricular canal is

demonstrated at the junction of the aortic root and the crest of the muscular interventricular septum (Figure 14.5G - asterisk).

Atrial Septation—The different components of the central cushion tissue contributing to atrial, ventricular, and atrioventricular septa are present in Figure 14.5H. Inferior and superior endocardial atrioventricular cushions are modified into the right tricuspid and left mitral septal valve leaflets, respectively. The vestibular spine (labeled as VS) serves as the attachment site for the septum primum and the right venous valve leaflet.

The second atrial septum, septum secundum, is a fold of atrial myocardium that has started to grow at E12.5 slightly right of the septum primum over the ostium secundum, and toward the atrioventricular cushion tissue (Figures 14.5H and 6C - SS). The lower border of the septum secundum (Figure 15.5A - SS) never completely fuses with the atrioventricular cushion, leaving an opening (Figure 14.5H). Though the common atrial chamber is divided in two by E14.0, there is considerable blood flow from the right to the left atrium during fetal development via this opening and the ostium secundum. This inter-atrial channel is called the foramen ovale, and it is formed in a way that the largely oxygenated blood entering into the right atrium through the inferior vena cava is directed across the midline into the cavity of the left atrium. The deoxygenated blood, which enters the rostral part of the right atrium through the right superior vena cava, is directed toward the right ventricle (Kaufman and Bard 1999) (Figure 7). The foramen ovale is normally closed at birth by the fusion of the two atrial septa (Webb et al. 1998).

Failure of adequate development of the septum primum or septum secundum results in an atrial septal defect (ASD), usually accompanied by defects in the mitral valve (Conway et al. 2003). At birth, failure of fusion of the atrial septa and subsequent closure of the inter-atrial shunt (the foramen ovale) may lead to death.

Ventricular Myocardium—The smooth zones of the interventricular septum and the pulmonary and aortic roots, compared to the trabeculated parts of the right and left ventricles, are recognizable (Figure 14.5G1). Compaction of the ventricular myocardium occurs between E13 and E14 (compare high-power images of the ventricular myocardium at these stages; 13.5H2 and 14.5G2), and this process is necessary to force generation and proper function of the ventricles in later fetal stages. The transition zone between compact and trabeculated tissues is called the spongy layer, and it is recognized as a network of fine trabeculations. The different layers of the ventricular myocardium can be distinguished as illustrated in Figures 14.5G1 and 14.5G2 (high magnification of 14.5G1 - CL, SL).

Noncompaction of the myocardium is associated with heart failure and sudden cardiac death.

E15.5 (TS24)-E18.5 (TS27)

Main developmental events:

Definitive external prenatal configuration achieved.

Atrioventricular valve leaflets are being modified

Coronary arteries are being modified

Modifications of Atrioventricular Valve Leaflets and Coronary Artery—Compared to earlier stages, the major changes apparent at E15.5 are an increase in the volume of the right atrium compared to that of the left atrium, and a change in orientation of the heart (Kaufman 1992). At E15.5 (Figure 8C), and even more apparent at E18.5 (Figures 9C and 18.5G), the axis of the heart becomes more oblique, and the ventricles, and more clearly the interventricular

septum, are being directed to the lower left part of the thoracic cavity. The heart has achieved its definitive prenatal configuration by E15.5, except for the atrioventricular valve leaflets and coronary artery.

Toward the ventricular apex, the atrioventricular valve leaflets are attached to the ventricular walls and interventricular septum through the developing papillary muscles (Figures 8D and 15.5D - PM) and chordae tendineae (Kruithof et al. 2007; Lincoln et al. 2004). Although endocardial atrioventricular cushions are important in the formation of atrioventricular valves, myocardial remodeling steps are necessary for subsequent maturation of the valve leaflets (Lamers et al. 1995; Wessels and Sedmera 2003). Between E15.5 and E18.5, the myocardium gradually disappears from the developing leaflets, resulting in thin, fibrous leaflets resembling the mature valve structures (Figures 15.5H and 18.5G - TVL, MVL). However, some condensation, elongation, and formation of nodular thickening and remodeling of the tension-resistant proteins will occur until postnatal day 11.5 (Kruithof et al. 2007). The tricuspid septal leaflet is one of the three leaflets that form the tricuspid valve. Development of the tricuspid septal leaflet (labeled as TSL) (Figure 18.5G) differs from that of the other leaflets in two ways. First, it is the only leaflet that delaminates from the interventricular septum (de Lange et al. 2004; Gaussin et al. 2005) and second, this step does not happen until the postnatal period (Kruithof et al. 2007). In humans, failure of the tricuspid valve septal leaflet to delaminate is characteristic of Ebstein's Anomaly.

Coronary vasculature supplying blood to the heart muscle develops from a pro-epicardium–derived endothelial plexus that envelops the heart in a temporospatial pattern (Kirby 2007). Just rostral to the aortic valve, at the region of the aortic sinuses (Figures 8B and 18.5E - AoS), the primitive coronary capillary plexus is gradually reduced to right and left, single intramyocardial definitive coronary arteries by about E16.5 (Kaufman and Bard 1999). Coronary arteries course along the ventricular borders to reach the heart apex, giving off small branches at perpendicular or acute angles to supply the ventricles. The ventricular septum is supplied by the septal artery, which arises as a main branch from the right coronary artery (Icardo and Colvee 2001).

A wide variety of anomalies in the origin and course of the coronary arteries has been reported within normal and mutant mice. These anomalies include single coronary artery, accessory coronary ostium, high takeoff, slit- or sinus-like ostium, and origin of the septal artery from the left coronary artery (Fernandez et al. 2008). Most coronary anomalies appear to be due to defective connections between the aortic root and the developing coronaries (Icardo and Colvee 2001). Though neural crest cells do not contribute structurally to the coronary arteries (Waldo et al. 1994), normal coronary artery development has been suggested to be dependent on a balance of cardiac neural crest cells and pro-epicardial cells (Li et al. 2002).

Discussion

This histology atlas was created to provide a detailed reference resource for identification of normal structures relevant to the most important developmental events in the embryonic/fetal mouse heart from E11.5 to E18.5. It is intended to assist pathologists and biomedical scientists in meeting the challenges of phenotyping the increasing number of mice with developmental cardiac abnormalities or in utero lethality, whether spontaneous or induced by chemicals or genetic modification.

Structural Differences between Human and Mouse Heart

Genetically modified mice, in which genes putatively important in cardiogenesis are targeted, are intended to serve as models of human congenital heart diseases. Apart from the obvious difference in size, anatomically, the mouse heart and the human heart are remarkably similar

throughout development (Wessels and Sedmera 2003). However, it is important to keep in mind that there are some morphological differences between the mouse and human in terms of developmental cardiac structures. The most marked differences are found in embryonic venous structures entering the atria. In the mouse, the left superior cava vena persists and drains to the coronary sinus, whereas in humans, this vessel is replaced by the brachiocephalic vein. The latter is connected to a right-sided superior vena cava, and the venous return from the upper body is via a single superior vena cava (Kaufman and Richardson 2005). In addition, the murine pulmonary vein enters the left atrium via a solitary opening; in contrast, there are four openings in humans (Kirby 2007; Webb et al. 1996).

Approach to Phenotyping Prenatal Cardiovascular Defects

Information presented at the gross examination of the embryo/fetus, along with the anatomic and histological details provided within this manuscript, can make the pathologist's task of analyzing and determining the cause of a cardiovascular problem more approachable. Not only the heart, but also the yolk sac, fetal vessels, umbilical vessels, and the tissue from which the heart and its structures are derived (endoderm and neural crest cells) should be considered when investigating a heart defect. The embryo/fetus should be inspected for evidence of diminished growth, the presence of anasarca, increased liver size secondary to blood engorgement, and pericardial sac distension. Typically, these gross findings are indicative of a heart deficiency. In addition, one should note if blood is present in the yolk sac vessels and if a heartbeat is present. After the gross examination, the entire embryo/fetus can be carefully dissected from the yolk sac and submitted for histological evaluation. It is recommended to submit the entire embryo when heart evaluation is desired, since a single heart insufficiency can lead to multiple secondary morphological and functional problems that may not be identified if just the heart was evaluated histologically. The histological exam can also be tackled in a systematic approach. Failure in heart specification or early differentiation can cause lethality before E9.5. After that time, insufficient cardiac function, structural defects, or conduction system defects can result in late-gestation death. Papaionnou and Behringer (2005) discuss these and other approaches to phenotypic analysis of prenatal lethality and postnatal effects. Evaluating mutant phenotypes in mice, whether they arise from a spontaneous mutation or targeted mutagenesis, requires the concepts and tools mentioned above as well as an atlas of normal histology with which to compare. Identification and evaluation of mutant phenotypes can ultimately aid in the understanding of how alterations in the genome result in complex changes in the organism and thus provide an understanding of gene control and function.

Acknowledgments

The authors wish to acknowledge Norris Flagler (NIEHS), Beth Mahler (EPL), and Elizabeth Ney (NIEHS) for image scanning and photographic assistance and David Sabio (EPL) for schematic illustrations. We are grateful to Dr. Matthew Kaufman, Dr. Dave Malarkey, Dr. Robert Maronpot, Dr. Yuji Mishina, and Dr. Kathy Sulik for their valuable comments while reviewing the manuscript.

Competing Interest: Financial support was provided to Dr. Savolainen by the Academy of Finland, Emil Aaltonen's Foundation, and Finnish Culture Foundation. This research was supported (in part) by the Intramural Research Program of the National Institutes of Health, National Institute of Environmental Health Sciences. The author has not declared any other competing interests.

References

Abdelwahid E, Pelliniemi LJ, Niinikoski H, Simell O, Tuominen J, Rahkonen O, Jokinen E. Apoptosis in the pattern formation of the ventricular wall during mouse heart organogenesis. Anat Rec 1999;256:208–17. [PubMed: 10486519]

Anderson RH, Brown NA, Moorman AF. Development and structures of the venous pole of the heart. Dev Dyn 2006;235:2–9. [PubMed: 16193508]

Brewer S, Jiang X, Donaldson S, Williams T, Sucov HM. Requirement for AP-2 in cardiac outflow tract morphogenesis. Mech Dev 2002;110:139–49. [PubMed: 11744375]

Chen TH, Chang TC, Kang JO, Choudhary B, Makita T, Tran CM, Burch JB, Eid H, Sucov HM. Epicardial induction of fetal cardiomyocyte proliferation via a retinoic acid-inducible trophic factor. Dev Biol 2002;250:198–207. [PubMed: 12297106]

Choudhary B, Ito Y, Makita T, Sasaki T, Chai Y, Sucov HM. Cardiovascular malformations with normal smooth muscle differentiation in neural crest-specific type II TGFbeta receptor (Tgfbr2) mutant mice. Dev Biol 2006;289:420–29. [PubMed: 16332365]

Conway SJ, Kruzynska-Frejtag A, Kneer PL, Machnicki M, Koushik SV. What cardiovascular defect does my prenatal mouse mutant have, and why? Genesis 2003;35:1–21. [PubMed: 12481294]

Copp AJ. Death before birth: clues from gene knockouts and mutations. Trends Genet 1995;11:87–93. [PubMed: 7732578]

Creazzo TL, Godt RE, Leatherbury L, Conway SJ, Kirby ML. Role of cardiac neural crest cells in cardiovascular development. Annu Rev Physiol 1998;60:267–86. [PubMed: 9558464]

DeHaan, RL. Morphogenesis of the vertebrate heart. In: Dehaan, RL.; Ursprung, H., editors. Organogenesis. Holt, Rinehart & Winston; New York: 1965. p. 377-419.

de Lange FJ, Moorman AF, Anderson RH, Manner J, Soufan AT, de Gier-de Vries C, Schneider MD, Webb S, van den Hoff MJ, Christoffels VM. Lineage and morphogenetic analysis of the cardiac valves. Circ Res 2004;95:645–54. [PubMed: 15297379]

Erokhina EL. Proliferation dynamics of cellular elements in the differentiating mouse myocardium. Tsitologiia 1968;10:1391–409. [PubMed: 5735190]

Fananapazir K, Kaufman MH. Observations on the development of the aortico-pulmonary spiral septum in the mouse. J Anat 1988;158:157–72. [PubMed: 3225220]

Farrell M, Waldo K, Li YX, Kirby ML. A novel role for cardiac neural crest in heart development. Trends Cardiovasc Med 1999;9:214–20. [PubMed: 10881754]

Fernandez B, Duran AC, Fernandez MC, Fernandez-Gallego T, Icardo JM, Sans-Coma V. The coronary arteries of the C57BL/6 mouse strains: implications for comparison with mutant models. J Anat 2008;212:12–18. [PubMed: 18067545]

Franco D, Campione M, Kelly R, Zammit PS, Buckingham M, Lamers WH, Moorman AF. Multiple transcriptional domains, with distinct left and right components, in the atrial chambers of the developing heart. Circ Res 2000;87:984–91. [PubMed: 11090542]

Gaussin V, Morley GE, Cox L, Zwijsen A, Vance KM, Emile L, Tian Y, Liu J, Hong C, Myers D, Conway SJ, Depre C, Mishina Y, Behringer RR, Hanks MC, Schneider MD, Huylebroeck D, Fishman GI, Burch JB, Vatner SF. Alk3/Bmpr1a receptor is required for development of the atrioventricular canal into valves and annulus fibrosus. Circ Res 2005;97:219–26. [PubMed: 16037571]

Gitler AD, Lu MM, Jiang YQ, Epstein JA, Gruber PJ. Molecular markers of cardiac endocardial cushion development. Dev Dyn 2003;228:643–50. [PubMed: 14648841]

Hiruma T, Nakajima Y, Nakamura H. Development of pharyngeal arch arteries in early mouse embryo. J Anat 2002;201:15–29. [PubMed: 12171473]

His W. Die area interposita, die Eustachische klappe und die spina vestibuli. Anatomie Menschlicher Embryonen 1880;1880:149–52.

Ho SY, Anderson RH. How constant anatomically is the tendon of Todaro as a marker for the triangle of Koch? J Cardiovasc Electrophysiol 2000;11:83–89. [PubMed: 10695467]

Hoffman JI, Kaplan S, Liberthson RR. Prevalence of congenital heart disease. Am Heart J 2004;147:425–39. [PubMed: 14999190]

Hurle JM, Colvee E, Blanco AM. Development of mouse semilunar valves. Anat Embryol (Berl) 1980;160:83–91. [PubMed: 7469038]

Icardo JM. Developmental biology of the vertebrate heart. J Exp Zool 1996;275:144–61. [PubMed: 8676095]

Icardo JM, Colvee E. Origin and course of the coronary arteries in normal mice and in iv/iv mice. J Anat 2001;199:473–82. [PubMed: 11693308]

Jacobson MD, Weil M, Raff MC. Programmed cell death in animal development. Cell 1997;88:347–54. [PubMed: 9039261]

Jiang X, Rowitch DH, Soriano P, McMahon AP, Sucov HM. Fate of the mammalian cardiac neural crest. Development 2000;127:1607–16. [PubMed: 10725237]

Kaufman, MH. The Atlas of Mouse Development. Academic Press; San Diego: 1992.

Kaufman, MH.; Bard, JBL. The Anatomical Basis of the Mouse Development. Academic Press; San Diego, CA: 1999.

Kaufman MH, Navaratnam V. Early differentiation of the heart in mouse embryos. J Anat 1981;133:235–46. [PubMed: 7333952]

Kaufman MH, Richardson L. 3D reconstruction of the vessels that enter the right atrium of the mouse heart at Theiler Stage 20. Clin Anat 2005;18:27–38. [PubMed: 15597370]

Kirby, M. The heart. In: Thorogood, P., editor. Embryos, Genes, and Birth Defects. Wiley & Sons; London, UK: 1997. p. 231-45.

Kirby ML. Molecular embryogenesis of the heart. Pediatr Dev Pathol 2002;5:516–43. [PubMed: 12297889]

Kirby, ML. Cardiac Development. Oxford University Press; New York: 2007.

Kirby ML, Gale TF, Stewart DE. Neural crest cells contribute to normal aorticopulmonary septation. Science 1983;220:1059–61. [PubMed: 6844926]

Kisanuki YY, Hammer RE, Miyazaki J, Williams SC, Richardson JA, Yanagisawa M. Tie2-Cre transgenic mice: a new model for endothelial cell-lineage analysis in vivo. Dev Biol 2001;230:230–42. [PubMed: 11161575]

Komiyama M, Ito K, Shimada Y. Origin and development of the epicardium in the mouse embryo. Anat Embryol (Berl) 1987;176:183–89. [PubMed: 3619072]

Kruithof BP, Krawitz SA, Gaussin V. Atrioventricular valve development during late embryonic and postnatal stages involves condensation and extracellular matrix remodeling. Dev Biol 2007;302:208–17. [PubMed: 17054936]

Kruithof BP, van den Hoff MJ, Wessels A, Moorman AF. Cardiac muscle cell formation after development of the linear heart tube. Dev Dyn 2003;227:1–13. [PubMed: 12701094]

Lamers WH, Viragh S, Wessels A, Moorman AF, Anderson RH. Formation of the tricuspid valve in the human heart. Circulation 1995;91:111–21. [PubMed: 7805192]

Li WE, Waldo K, Linask KL, Chen T, Wessels A, Parmacek MS, Kirby ML, Lo CW. An essential role for connexin43 gap junctions in mouse coronary artery development. Development 2002;129:2031–42. [PubMed: 11934868]

Lincoln J, Alfieri CM, Yutzey KE. Development of heart valve leaflets and supporting apparatus in chicken and mouse embryos. Dev Dyn 2004;230:239–50. [PubMed: 15162503]

Lyons GE, Schiaffino S, Sassoon D, Barton P, Buckingham M. Developmental regulation of myosin gene expression in mouse cardiac muscle. J Cell Biol 1990;111:2427–36. [PubMed: 2277065]

Markwald RR, Fitzharris TP, Manasek FJ. Structural development of endocardial cushions. Am J Anat 1977;148:85–119. [PubMed: 842477]

Mjaatvedt CH, Markwald RR. Induction of an epithelialmesenchymal transition by an in vivo adheron-like complex. Dev Biol 1989;136:118–28. [PubMed: 2509260]

Molin DG, DeRuiter MC, Wisse LJ, Azhar M, Doetschman T, Poelmann RE, Gittenberger-de Groot AC. Altered apoptosis pattern during pharyngeal arch artery remodelling is associated with aortic arch malformations in Tgfbeta2 knock-out mice. Cardiovasc Res 2002;56:312–22. [PubMed: 12393102]

Papaioannou, V.; Behringer, R. Mouse Phenotypes A Handbook of Mutation Analysis. Cold Spring Harbor Laboratory Press; New York: 2005.

Perez-Pomares JM, Macias D, Garcia-Garrido L, Munoz-Chapuli R. Contribution of the primitive epicardium to the subepicardial mesenchyme in hamster and chick embryos. Dev Dyn 1997;210:96–105. [PubMed: 9337131]

Petiet A, Kaufman M, Goddeeris M, Brandenburg J, Elmore S, Johnson GA. High-resolution magnetic resonance histology of the embryonic and neonatal mouse: a 4D atlas and morphologic database. Proc Natl Acad Sci U S A 2008;105:12331–36. [PubMed: 18713865]

Pexieder T. Cell death in the morphogenesis and teratogenesis of the heart. Adv Anat Embryol Cell Biol 1975;51:3–99. [PubMed: 50000]

Pexieder, T. Conotruncus and Its Septation at the Advent of the Molecular Biology Era. In: Clark, EB.; Markwald, RR.; Takao, A., editors. Developmental Mechanisms of Heart Disease. Futura Publishing Co., Inc.; New York: 1995. p. 227-47.

Phillips MT, Kirby ML, Forbes G. Analysis of cranial neural crest distribution in the developing heart using quail-chick chimeras. Circ Res 1987;60:27–30. [PubMed: 3568286]

Poelmann RE, Gittenberger-de Groot AC. Apoptosis as an instrument in cardiovascular development. Birth Defects Res C Embryo Today 2005;75:305–13. [PubMed: 16425248]

Poelmann RE, Molin D, Wisse LJ, Gittenberger-de Groot AC. Apoptosis in cardiac development. Cell Tissue Res 2000;301:43–52. [PubMed: 10928280]

Rajagopal SK, Ma Q, Obler D, Shen J, Manichaikul A, Tomita-Mitchell A, Boardman K, Briggs C, Garg V, Srivastava D, Goldmuntz E, Broman KW, Woodrow Benson D, Smoot LB, Pu WT. Spectrum of heart disease associated with murine and human GATA4 mutation. J Mol Cell Cardiol 2007;43:677–85. [PubMed: 17643447]

Song L, Yan W, Chen X, Deng CX, Wang Q, Jiao K. Myocardial smad4 is essential for cardiogenesis in mouse embryos. Circ Res 2007;101:277–85. [PubMed: 17585069]

Soufan AT, van den Hoff MJ, Ruijter JM, de Boer PA, Hagoort J, Webb S, Anderson RH, Moorman AF. Reconstruction of the patterns of gene expression in the developing mouse heart reveals an architectural arrangement that facilitates the understanding of atrial malformations and arrhythmias. Circ Res 2004;95:1207–15. [PubMed: 15550689]

Sulik, KK.; Bream, PRJ. Educational Technology Group, University of North Carolina; Chapel Hill: 1999. Embryo images: normal & abnormal mammalian development. Available at: http://www.med.unc.edu/embryo_images/unit-welcome/welcome_htms/akgs.htm

Theiler, K. The House Mouse: Development and Normal Stages from Fertilization to 4 weeks of Age. Springer-Verlag; Berlin: 1972.

Theiler, K. The House Mouse: Atlas of Mouse Development. Springer-Verlag; New York: 1989.

Thompson RP, Abercrombie V, Wong M. Morphogenesis of the truncus arteriosus of the chick embryo heart: movements of autoradiographic tattoos during septation. Anat Rec 1987;218:394–95. 434.

van den Hoff MJ, Kruithof BP, Moorman AF. Making more heart muscle. Bioessays 2004;26:248–61. [PubMed: 14988926]

Vuillemin M, Pexieder T. Normal stages of cardiac organogenesis in the mouse: II. Development of the internal relief of the heart. Am J Anat 1989;184:114–28. [PubMed: 2712003]

Waldo K, Miyagawa-Tomita S, Kumiski D, Kirby ML. Cardiac neural crest cells provide new insight into septation of the cardiac outflow tract: aortic sac to ventricular septal closure. Dev Biol 1998;196:129–44. [PubMed: 9576827]

Waldo KL, Kumiski DH, Kirby ML. Association of the cardiac neural crest with development of the coronary arteries in the chick embryo. Anat Rec 1994;239:315–31. [PubMed: 7943763]

Waldo KL, Lo CW, Kirby ML. Connexin 43 expression reflects neural crest patterns during cardiovascular development. Dev Biol 1999;208:307–23. [PubMed: 10191047]

Watanabe M, Choudhry A, Berlan M, Singal A, Siwik E, Mohr S, Fisher SA. Developmental remodeling and shortening of the cardiac outflow tract involves myocyte programmed cell death. Development 1998;125:3809–20. [PubMed: 9729489]

Webb S, Anderson RH, Lamers WH, Brown NA. Mechanisms of deficient cardiac septation in the mouse with trisomy 16. Circ Res 1999;84:897–905. [PubMed: 10222336]

Webb S, Brown NA, Anderson RH. The structure of the mouse heart in late fetal stages. Anat Embryol (Berl) 1996;194:37–47. [PubMed: 8800421]

Webb S, Brown NA, Anderson RH. Formation of the atrioventricular septal structures in the normal mouse. Circ Res 1998;82:645–56. [PubMed: 9546373]

Webb S, Qayyum SR, Anderson RH, Lamers WH, Richardson MK. Septation and separation within the outflow tract of the developing heart. J Anat 2003;202:327–42. [PubMed: 12739611]

Wessels A, Markwald R. Cardiac morphogenesis and dysmorphogenesis. I. Normal development. Methods Mol Biol 2000;136:239–59. [PubMed: 10840715]

Wessels A, Sedmera D. Developmental anatomy of the heart: a tale of mice and man. Physiol Genomics 2003;15:165–76. [PubMed: 14612588]

Yelbuz TM, Waldo KL, Kumiski DH, Stadt HA, Wolfe RR, Leatherbury L, Kirby ML. Shortened outflow tract leads to altered cardiac looping after neural crest ablation. Circulation 2002;106:504–10. [PubMed: 12135953]

Abbreviations

AA	aortic arch arteries
AAo	ascending aorta
Ao	aortic trunk
AoS	aortic sinuses
AR	aortic root (vestibule)
ARL	accessory lobe of right lung
AS	aortic sac
ASD	atrial septal defect
AVC	atrioventricular canal
AVL	aortic valve leaflet
AVS	atrioventricular septum
AVSD	atrioventricular septal defect
BC	bulbus cordis
BVC	bulboventricular canal
BVG	bulboventricular groove
CAC	common atrial chamber
CAP	mesenchymal cap of the SP
CAVC	complete AV canal
CL	compact layer
COS	conal septum
CT	cushion tissue
DA	ductus arteriosus
Dao	descending aorta
DILV	double inlet left ventricle
DoA	dorsal aorta
DORV	double outlet right ventricle
DPC	days post-conception

E	esophagus
E7.5–18.5	embryonic day 7.5–18.5
ECCD	endocardial cushion defect
H&E	hematoxylin and eosin
IAC	inferior atrioventricular cushion
IVC	inferior vena cava
IVS	interventricular septum
LA	left atrium
LACV	left anterior cardinal vein
LAVC	left atrioventricular canal
LCCV	left common cardinal vein
LLAC	left lateral atrioventricular cushion
LSV	left superior vena cava
LV	left ventricle
MB	main bronchus
MVL	mitral valve leaflet
OCT	outflow tract cushion tissue
OFT	outflow tract
OP	ostium primum
OS	ostium secundum
PA	pulmonary artery
PAA	pharyngeal arch artery
PBS	phosphate buffered saline
PC	pericardium
PCC	pericardial cavity
PLV	primitive (left) ventricle
PM	papillary muscle
PR	pulmonary root (infundibulum)
PRV	primitive right ventricle
PT	pulmonary trunk
PTA	persistent truncus arteriosus
PVe	pulmonary vein

PVL	pulmonary valve leaflet
RA	right atrium
RACV	right anterior cardinal vein
RAVC	right atrioventricular canal
RCCV	right common cardinal vein
RLAC	right lateral atrioventricular cushion
RPA	right pulmonary artery
RSV	right superior vena cava
RV	right ventricle
SAC	superior atrioventricular cushion tissue
SL	spongy layer
SP	septum primum
SS	septum secundum
SSp	septum spurium
SV	sinus venosus
T	trachea
TGA	transposition of great arteries
Th	left and right thymic primordial
TS	Theiler stage
TSL	tricuspid septal leaflet
TVL	tricuspid valve leaflet
VS	vestibular spine
VSD	ventricular septal defect
VV	venous valve
WAVC	wall of atrioventricular canal

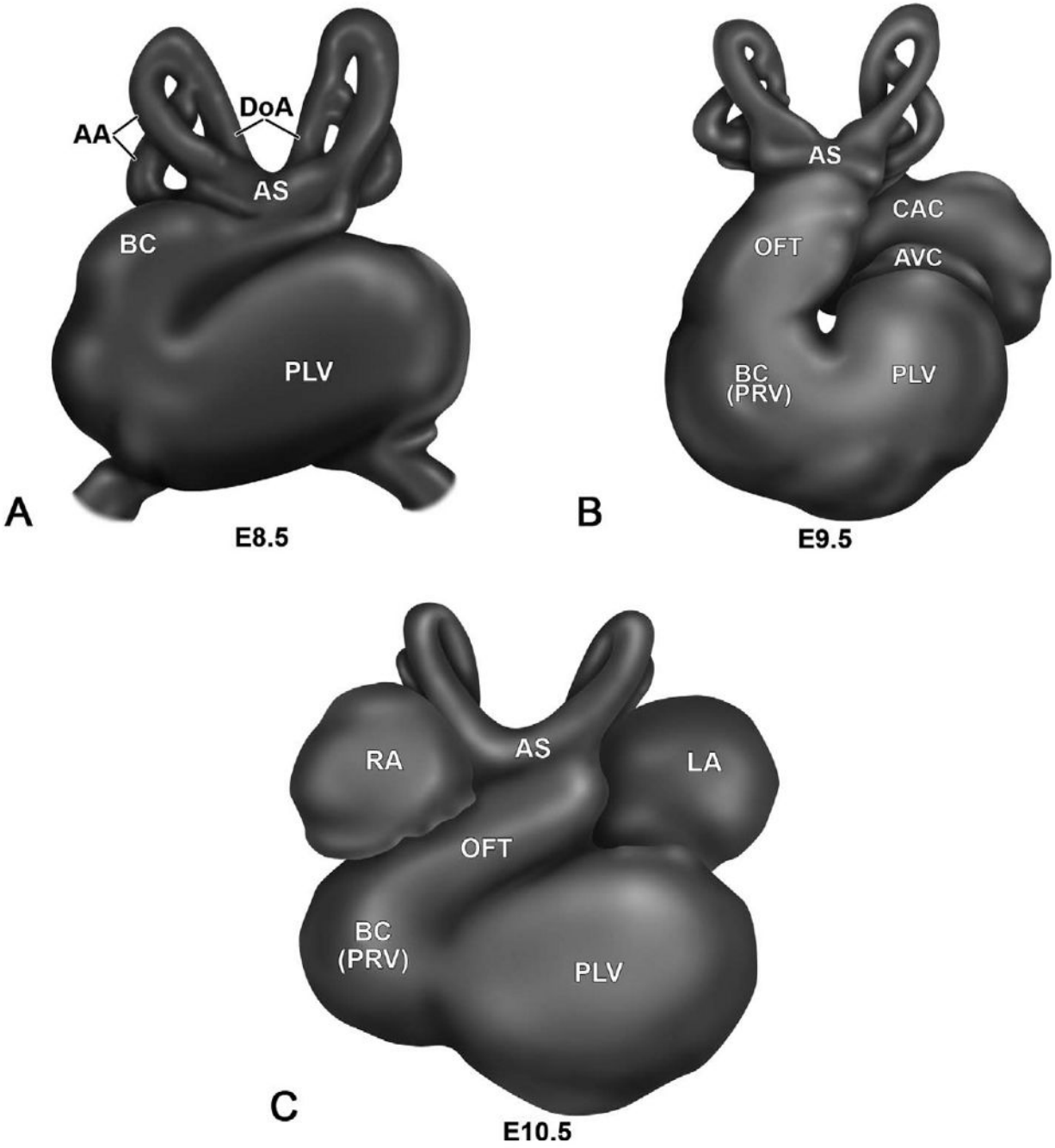

Figure 1.

Early cardiovascular development of the mouse. The schematic illustrations of the mouse heart from E8.5 (A), E9.5 (B) and E10.5 (C) illustrate the early developmental events of the cardiogenesis. The aortic sac (AS) contributes to the aortic arch arteries (AA), and the bulbus cordis (BC) mainly to the primitive right ventricle (PRV). AVC, atrioventricular canal; CAC, common atrial chamber; DoA, dorsal aorta; LA, (future) left atrium; OFT, outflow tract; PLV, primitive left ventricle; RA, (future) right atrium. Modified from Kirby M. (1997).

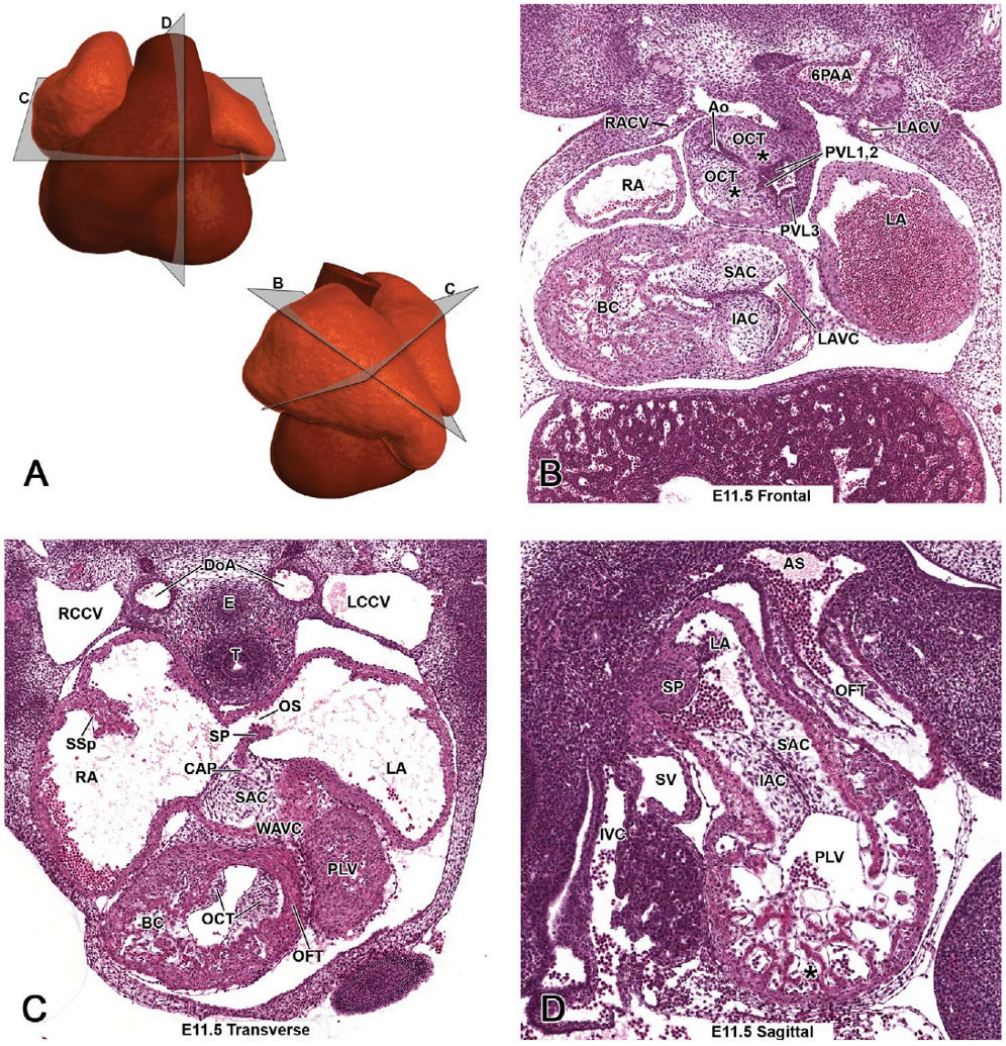

Figure 2.

Representative images of the E11.5 mouse heart. (A, upper panel) Schematic illustration of the E11.5 heart from a ventral view demonstrating the estimated planes corresponding to the site of the hematoxylin and eosin (H&E)-stained transverse (C) and sagittal (D) sections. (A, lower panel) Schematic illustration of the left lateral view demonstrates the heart of the E11.5 mouse, and is used here to show the estimated planes corresponding to the sites of H&E-stained E11.5 frontal (B) and transverse (C) sections. Main developmental events at E11.5 are the progressive septations of the common outflow tract, atria, and ventricles. Asterisks in B demonstrate the aortico-pulmonary septation complex within the outflow tract cushions.

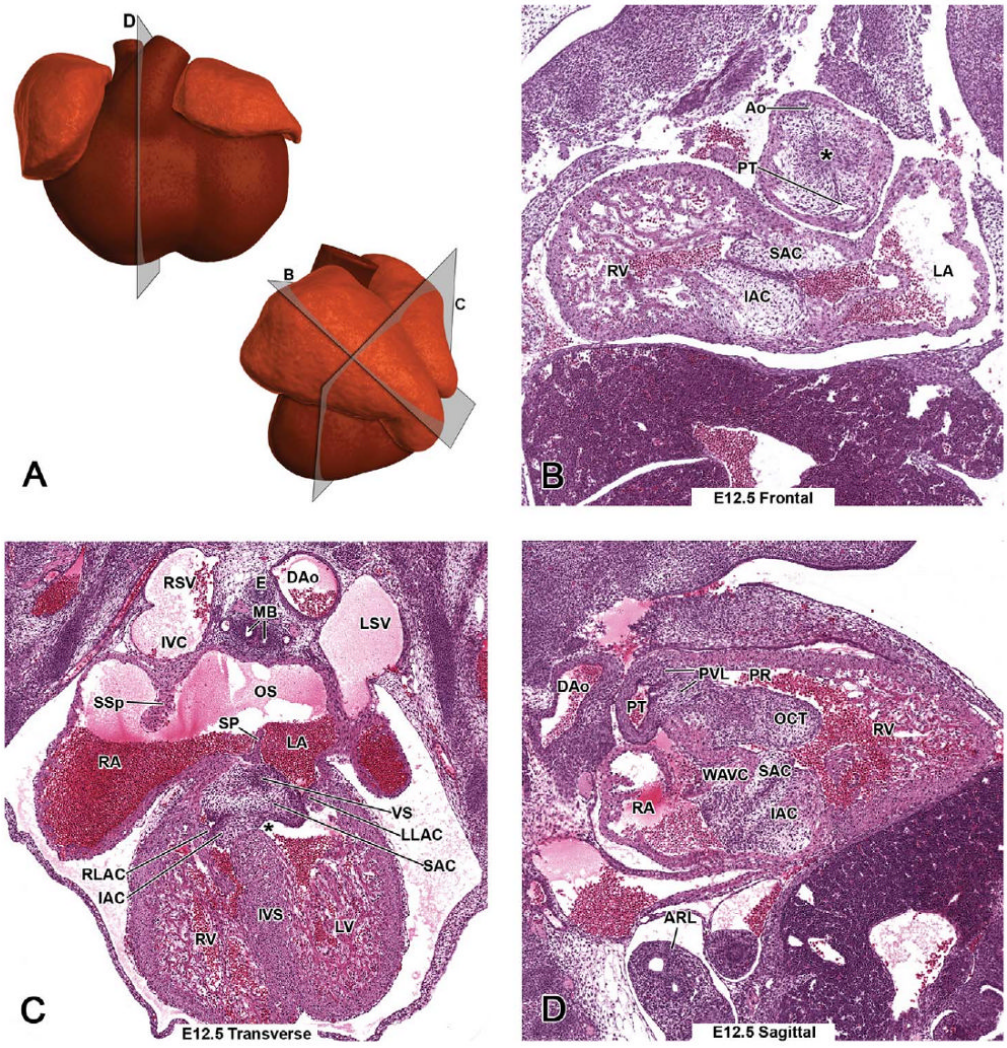

Figure 3.

Representative images of the E12.5 mouse heart. (A, upper panel) Schematic illustration of the E12.5 heart from a ventral view demonstrating the estimated plane corresponding to the site of the hematoxylin and eosin (H&E)-stained sagittal section (D). (A, lower panel) A schematic illustration of the left lateral view demonstrates the heart of the E12.5 mouse, and it is used here to show the estimated planes corresponding to the sites of H&E-stained E12.5 frontal (B) and transverse (C) sections. Main developmental events at E12.5 are the progressive septations of the common outflow tract, atria, and ventricles, and initiation of atrioventricular canal septation. An asterisk in B demonstrates the aorticopulmonary septation complex within the outflow tract cushions.

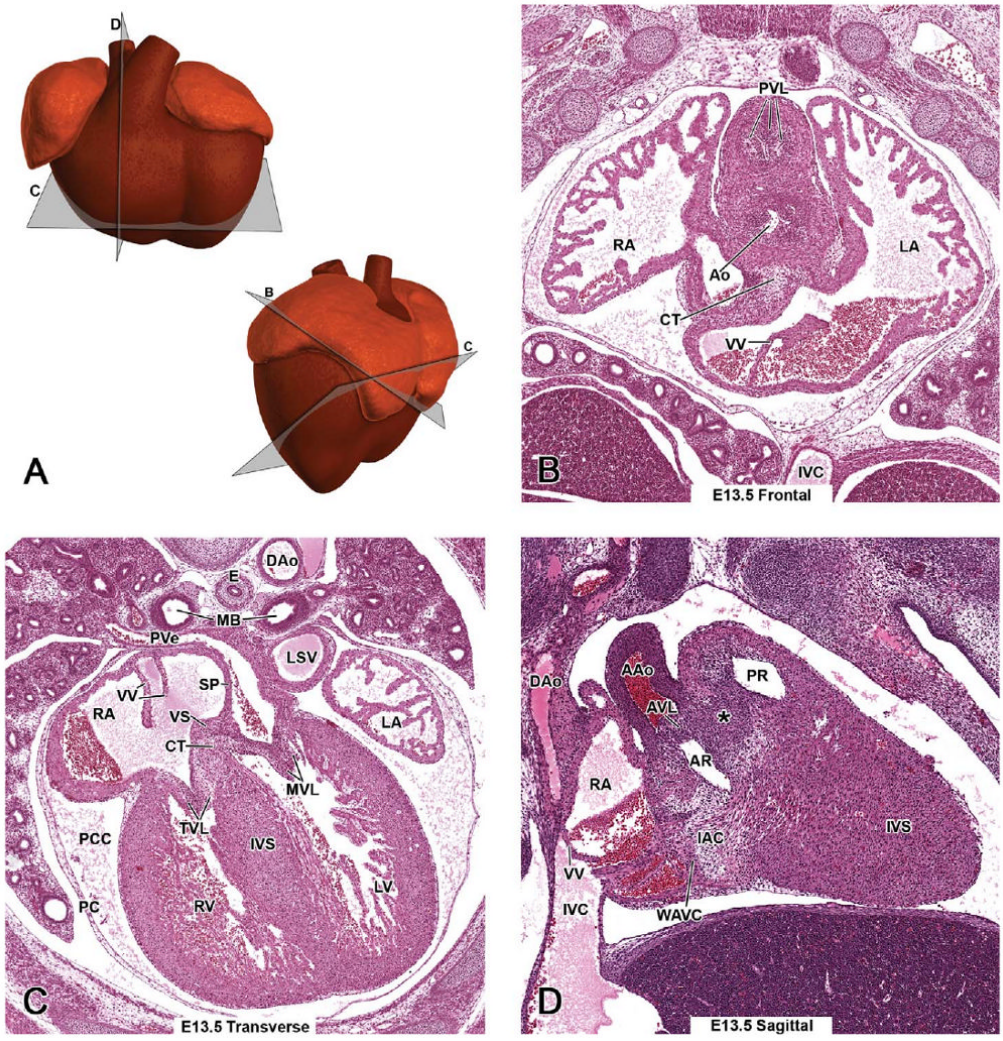

Figure 4.

Representative images of the E13.5 mouse heart. (A, upper panel) Schematic illustration of the E13.5 heart from a ventral view demonstrating the estimated planes corresponding to the sites of the hematoxylin and eosin (H&E)-stained transverse (C) and sagittal (D) sections. (A, lower panel) Schematic illustration of the E13.5 heart from a left lateral view demonstrating the estimated planes corresponding to the sites of H&E-stained E13.5 frontal (B) and transverse (C) sections. At E13.5, the common outflow tract and ventricles have been septated, but the atrial and atrioventricular septa are still under formation. An asterisk in D demonstrates the fibrous raphe at the site of fusion of the conal OFT ridges in the wall between the pulmonary and aortic roots.

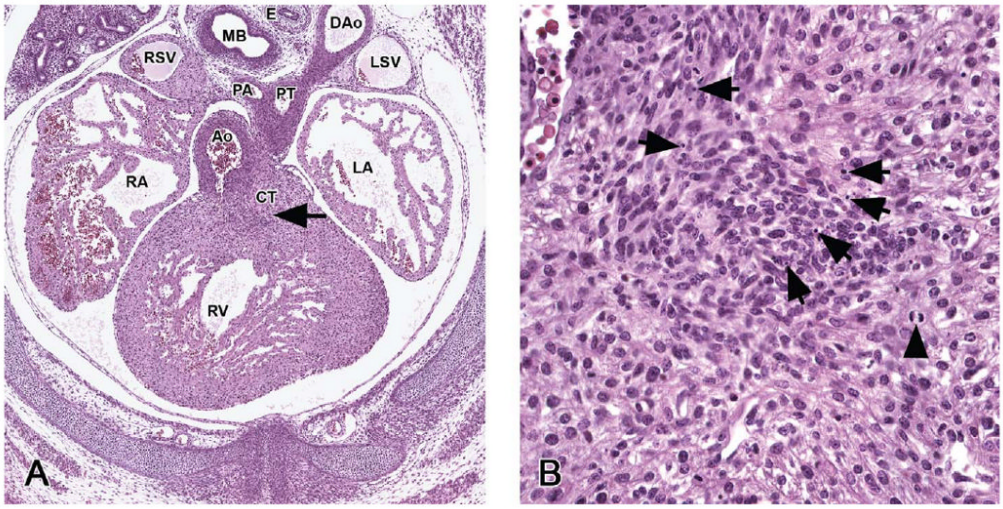

Figure 5.

Apoptosis in the outflow tract cushions of the E13.5 mouse heart. (A) A transverse section through the developing heart demonstrates the newly formed conal septum (arrow) separating the two ventricular outlets, pulmonary trunk, and aorta. (B) Foci of apoptotic cell debris (arrows) are found in the cushion tissue surrounding the newly formed conal septum. A mitotic cell (arrowhead) is also present.

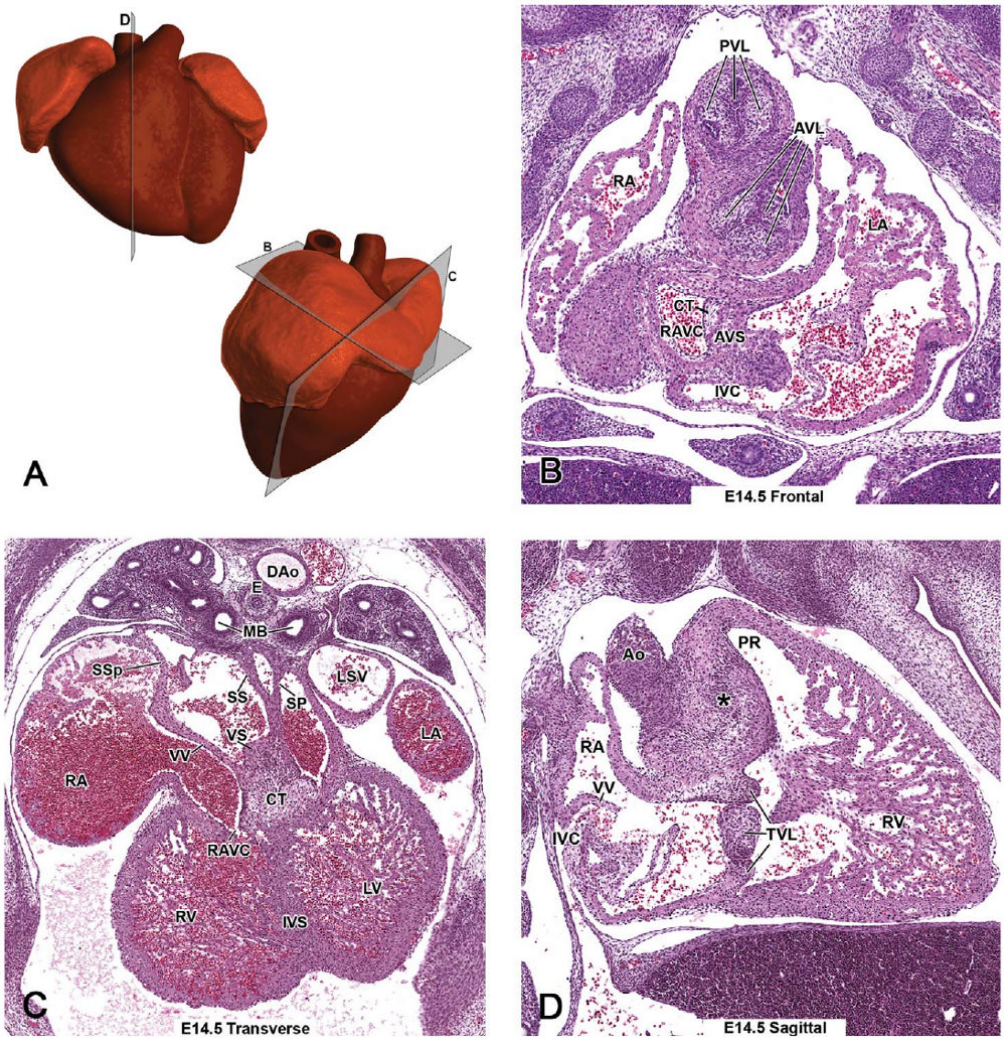

Figure 6.

Representative images of the E14.5 mouse heart. (A, upper panel) Schematic illustration of the E14.5 heart from a left ventral view demonstrating the estimated plane corresponding to the site of the hematoxylin and eosin (H&E)-stained sagittal section (D). (A, lower panel) Schematic illustration of the left lateral view demonstrates the heart of the E14.5 mouse, and it is used here to show the estimated planes corresponding to the sites of H&E-stained E14.5 frontal (B) and transverse (C) sections. At E14.5, the atrial septa have formed. An asterisk in D demonstrates the fibrous raphe at the site of fusion of the conal OFT ridges in the wall between the pulmonary and aortic roots.

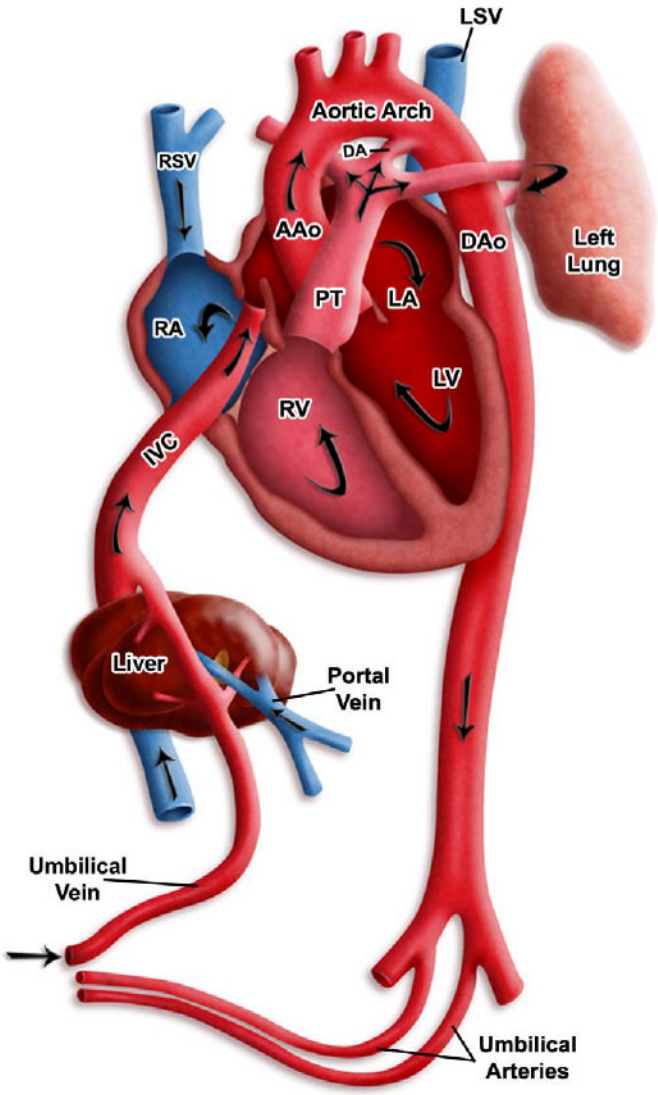

Figure 7.

A diagram displaying the blood flow in the heart of a late prenatal mouse. Oxygenated blood from the placenta that enters the right atrium is shunted through the inter-atrial septa via the foramen ovale to the left atrium, and through the left atrioventricular canal to the left ventricle. From there the blood is pumped out through the aorta. Deoxygenated blood, which enters the rostral part of the right atrium through the right superior vena cava, is directed toward the right ventricle. From there the blood is pumped through the pulmonary artery. Since the lungs are not yet functional and the resistance is high in the right and left pulmonary arteries, the majority of the blood is shunted through the ductus arteriosus into the descending aorta. At birth, the prenatal shunts, the foramen ovale, and the ductus arteriosus, are closed and separate pulmonary and systemic circulations are formed. Modified from Sadler T. M. (2000). Langman's Medical Embryology. S. Katz, ed.) p. 253. Lippincott Williams & Wilkins, Baltimore, MD.

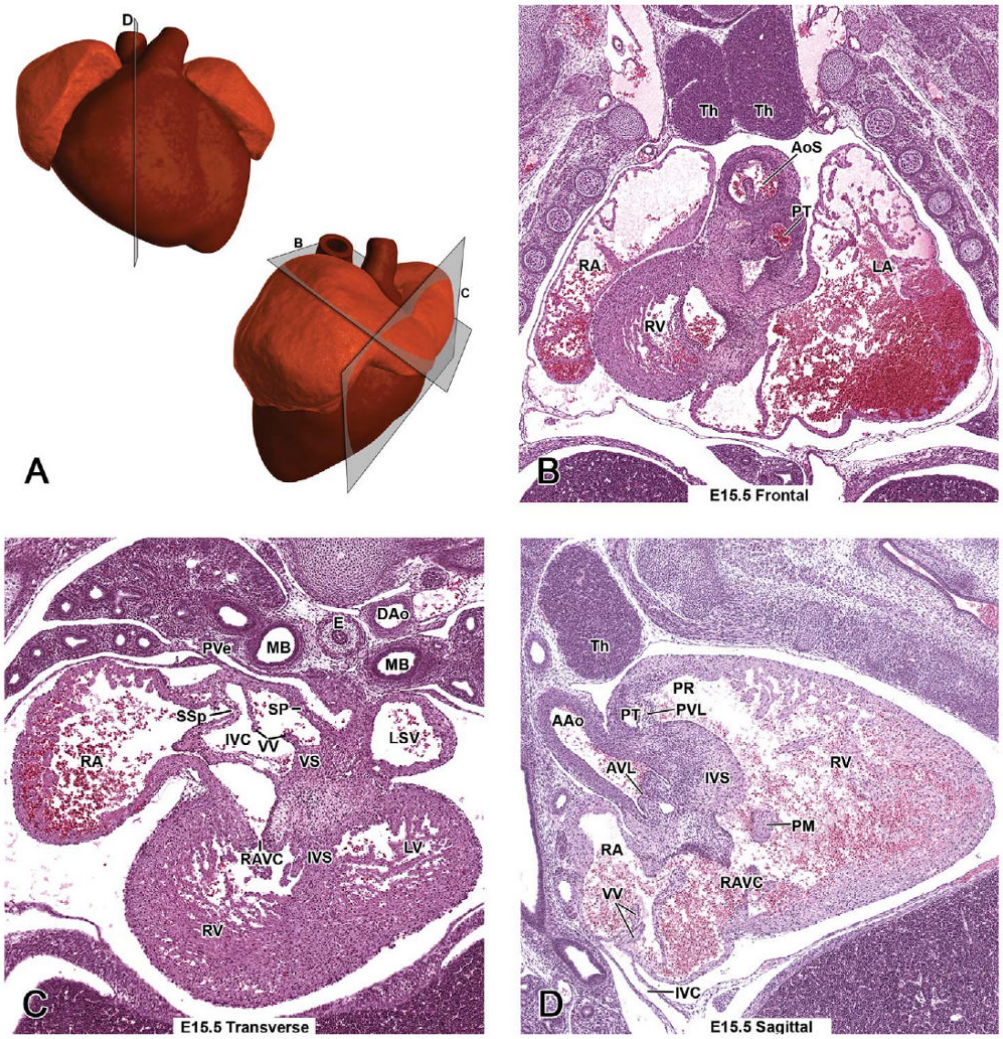

Figure 8.

Representative images of the E15.5 mouse heart. (A, upper panel) A schematic illustration of the E15.5 heart from a ventral view demonstrating the estimated planes corresponding to the site of the hematoxylin and eosin (H&E)-stained sagittal section (D). (A, lower panel) Schematic illustration of the left lateral view demonstrates the heart of the E15.5 mouse, and it is used here to show the estimated planes corresponding to the sites of H&E-stained E15.5 frontal (B) and transverse (C) sections. At E15.5, the heart has achieved its definitive external prenatal configuration; the atrioventricular valve leaflets and coronary arteries are being modified until after birth.

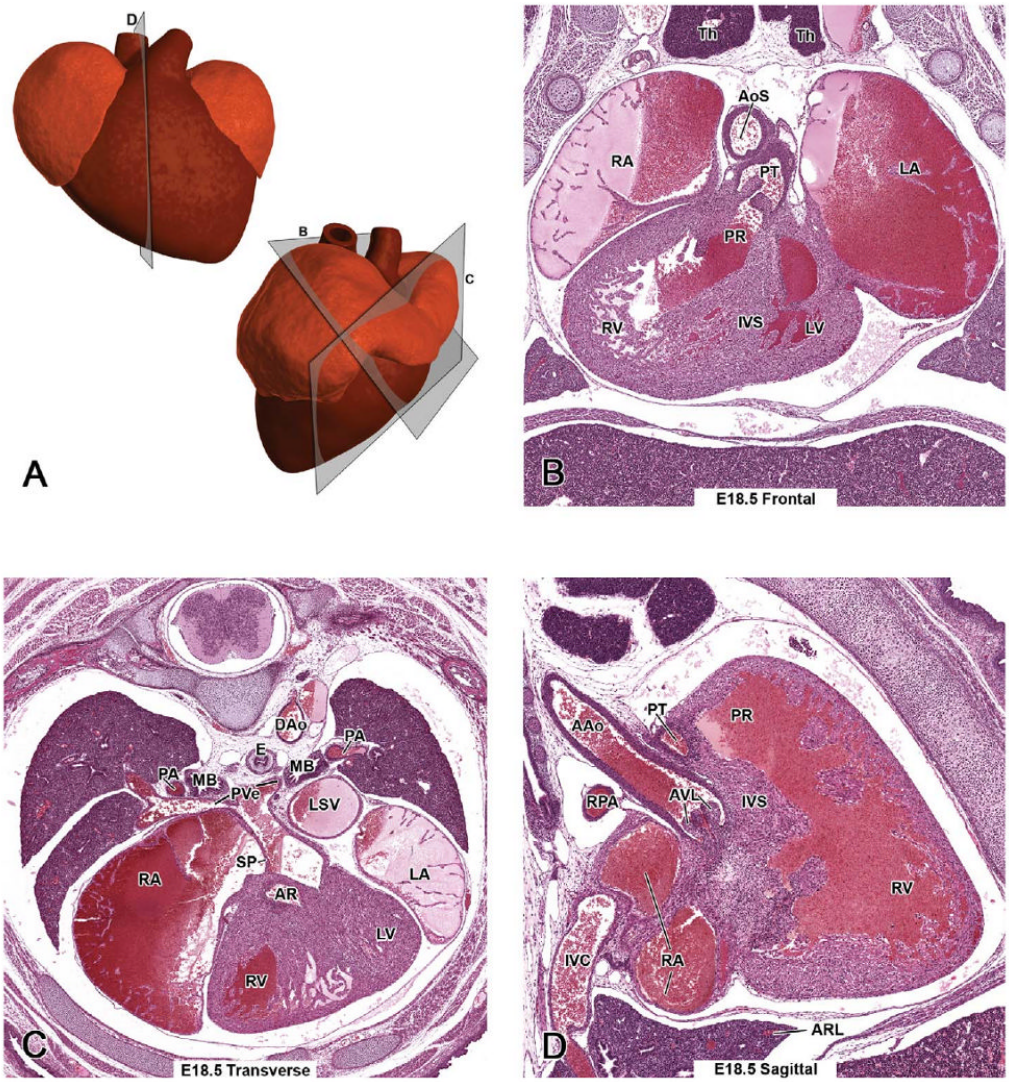

Figure 9.

Representative images of the E18.5 mouse heart. (A, upper panel) A schematic illustration of the E18.5 heart from a ventral view demonstrates the estimated plane corresponding to the hematoxylin and eosin–stained sagittal section (D). (A, lower panel) An illustration of the left lateral view of the E15.5 mouse heart is used to show the estimated planes of E18.5 frontal (B) and transverse (C) sections, because at E15.0 the heart has achieved its definite external prenatal configuration, and after that it only grows in size.

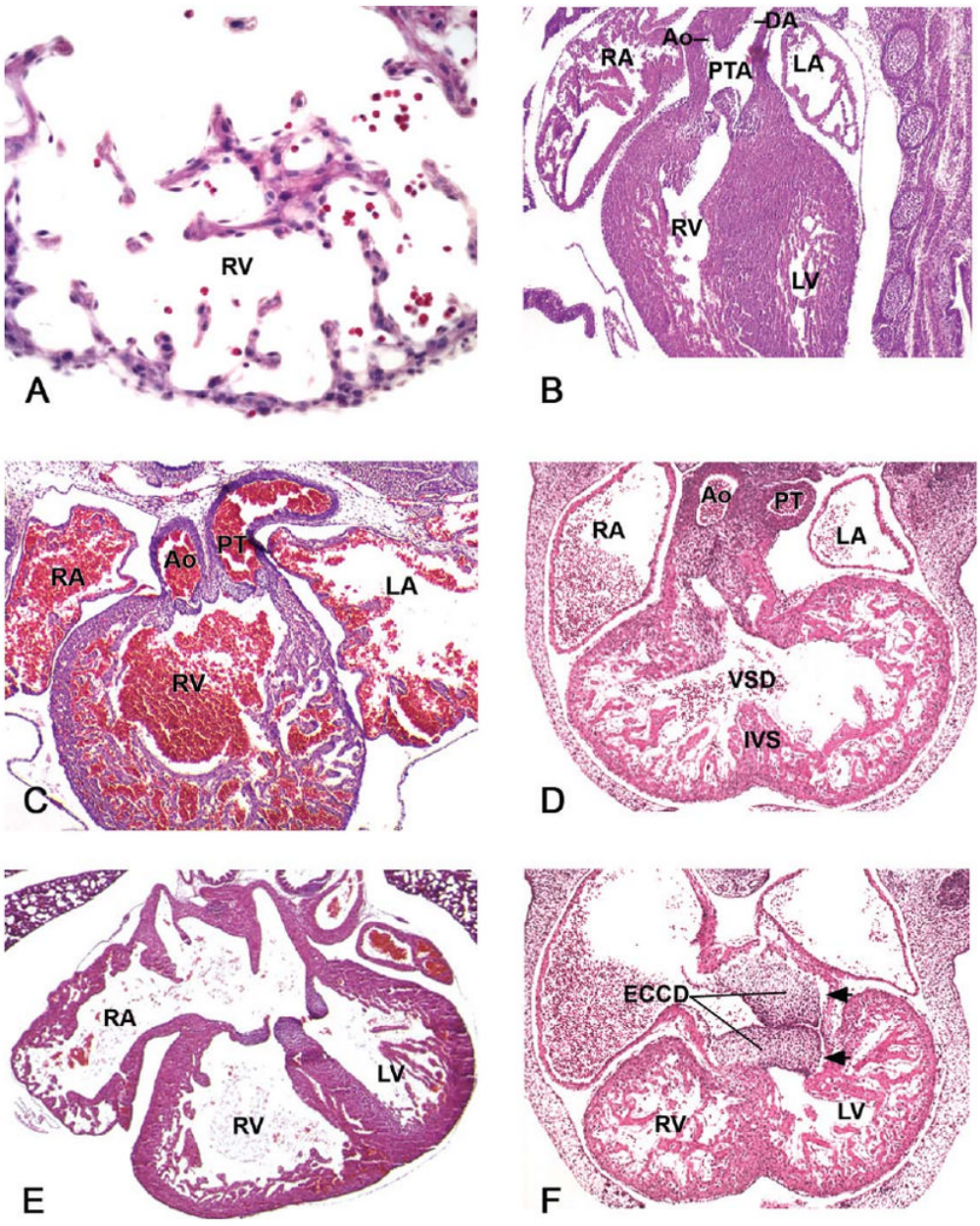

Figure 10.

Developmental cardiac lesions in prenatal mutant mice. (A) Hypocellular myocardial wall defect in E12.5 myocardial *Smad4*-deficiant mice. This high-power image is from the right ventricular (RV) wall. (B) A single outflow vessel, persistent truncus arteriosus (PTA), which branches distal to the outflow valve leaflets into the ascending aorta (Ao) and ductus arteriosus (DA) in E14.5 *Wnt1cre/Tgfbr2* mutant embryo. (C) Double-outlet right ventricle (DORV) in E15.5 AP-2α-deficient embryo. (D) Ventricular septal defect (VSD) with overriding aorta, a defect in which the malaligned root of the aorta is positioned over the VSD, in an E13.5 *Zfpm2*-deficient embryo. (E, F) Endocardial cushion defects (ECCD) may affect all of the components derived from it (atrioventricular valves, atrial and interventricular septa, IVS). Figure 10E describes a well-balanced common atrioventricular canal defect in a *GATA4* +/- late-gestation embryo, whereas in Figure 10F, a single poorly formed, left-sided common

atrioventricular valve that connects both atria to the left ventricle (LV) is apparent in an E13.5 *Zfpm2*-deficient embryo. The inlets are indicated with arrows. LA, left atrium; PT, pulmonary trunk; RA, right atrium. Figure 10A reprinted from: Song, L., Yan, W., Chen, X., Deng, C. X., Wang, Q., and Jiao, K. (2007). Myocardial Smad4 is Essential for Cardiogenesis in Mouse Embryos. *Circ Res* **101**, 277–85, with permission from Lippincott, Williams & Wilkins. Figure 10B reprinted from: Choudhary, B., Ito, Y., Makita, T., Sasaki, T., Chai, Y., and Sucov, H. M. (2006). Cardiovascular malformations with normal smooth muscle differentiation in neural crest-specific type II TGFbeta receptor (Tgfbr2) mutant mice. *Dev Biol* **289**, 420–29, with permission from Elsevier. Figure 10C reprinted from: Brewer, S., Jiang, X., Donaldson, S., Williams, T., and Sucov, H. M. (2002). Requirement for AP-2α in cardiac outflow tract morphogenesis. *Mech Dev* **110**, 139–49, with permission from Elsevier. Figures 10D and 10F: figures were kindly provided by Professor E. C. Svensson, University of Chicago. Figure 10E reprinted from: Rajagopal, S. K., Ma, Q., Obler, D., Shen, J., Manichaikul, A., Tomita-Mitchell, A., Boardman, K., Briggs, C., Garg, V., Srivastava, D., Goldmuntz, E., Broman, K. W., Woodrow Benson, D., Smoot, L. B., and Pu, W. T. (2007). Spectrum of heart disease associated with murine and human GATA4 mutation. *J Mol Cell Cardiol* **43**, 677–85, with permission from Elsevier.

Table 1

The most common abnormal cardiovascular phenotypes found in mutant pre- or perinatal mice.

Cardiovascular/cardiac phenotype	Number of genotypes with a certain phenotype
Abnormal heart septum morphology	**250**
*Abnormal ventricular septum morphology (VSD)**	*217*
Abnormal atrial septum morphology (ASD)	*76*
Abnormal outflow tract development	**147**
*Abnormal OFT septation (PTA)**	*87*
*Malalignment of the great vessels (DORV)**	*28*
Abnormal cardiac valve morphology	**134**
*Abnormal atrioventricular valve morphology (Atresia of mitral/tricuspid valve)**	*71*
Abnormal semilunar valve morphology	*66*
Heart valve hyperplasia	*5*
Abnormal myocardial trabeculae morphology	**126**
Poorly developed ventricular trabeculae	*57*
Absent myocardial trabeculae	*24*
Abnormal aortic arch/aorta morphology	**87/32**
Abnormal patterning of the aortic arch	*29*
Interrupted aortic arch	*28*
Right aortic arch	*28*
Retroesophageal right subclavian artery	*22*
*Overriding aorta**	*23*
Double aortic arch	*10*
Coarctation of aorta	*9*
Cervical aortic arch	*4*
Abnormal looping	**103**
Abnormal direction of looping	*36*
Failure of looping	*30*
Thin myocardial wall*	**70**
Abnormal endocardial cushion	**66**
Absent endocardial cushion	*18*
*Decreased endocardial cushion size (CAVC)**	*9*
Failure of endocardial cushion closure	*8*
Increased endocardial cushion size	*5*
Abnormal heart tube morphology	**47**
Cardia bifida	*10*
Abnormal atrioventricular canal	**32**
Dextrocardia (cardiac apex pointing to the right as opposed to the normal levocardia)	**19**
Abnormal pulmonary trunk morphology	**12**
Mesocardia (cardiac apex pointing to the middle as opposed to the normal levocardia)	**6**
Abnormal sinus venosus	**6**

Main categories of cardiovascular phenotypes are indicated in bold, and subcategories are italicized. The number of genotypes with a certain cardiovascular phenotype is indicated. One genotype may have several different cardiac abnormalities. The most common defects within categories are mentioned in parentheses. Cardiac defects marked with an asterisk are demonstrated in Figure 10. These data were collected from the Mouse Genome Database (MGD), Mouse Genome Informatics web site, The Jackson Laboratory, Bar Harbor, Maine (http://www.informatics.jax.org), February 2008.

Abbreviations: ASD, atrial septal defect; CAVC, common atrioventricular canal; DORV, double outlet right ventricle; PTA, persistent truncus arteriosus; VSD, ventricular septal defect.